

Probing Geometry with Stability Conditions

Paul S. Aspinwall

Center for Geometry and Theoretical Physics, Box 90318
Duke University, Durham, NC 27708-0318

Abstract

The notion that the geometry of spacetime is given by the moduli space of 0-branes is examined in four examples of Calabi–Yau threefolds. An important consideration when determining the moduli space of D-branes is the stability condition and this is key in our analysis. In the first two examples, the flop and the orbifold blowup, no surprises are found. Next, an exoflop is considered where the linear sigma model implies a \mathbb{P}^1 external to the Calabi–Yau threefold is part of the geometry. The 0-brane probe sees no such external \mathbb{P}^1 and furthermore exhibits a surprising discontinuity when following an extremal transition associated to the exoflop. Finally we consider a hybrid model of a Landau–Ginzburg fibration over a \mathbb{P}^1 . Using the technology of matrix factorizations we find a D-brane probe whose moduli space is this \mathbb{P}^1 but it is not a 0-brane and is not stable at the large radius limit of the Calabi–Yau manifold.

1 Introduction

Spacetime is supposed to be “emergent” in string theory. The notion of D-branes in the worldsheet description of string theory is one way to achieve this idea. If one has a perfect knowledge of the worldsheet physics then one should understand all possible boundary conditions, i.e., D-branes in the classical (zero string coupling) limit. Picking a suitable class of D-brane as a candidate 0-brane one can then try to construct a moduli space for all D-branes in this class. This resulting space should be spacetime.

The resulting spacetime is not unique. As is well known, there can be different choices of the class of a 0-brane and this leads to T-dual target spaces.

In the case of B-type topological field theories with target space a compact Calabi–Yau threefold X , the set of D-branes is given by the bounded derived category, $\mathbf{D}(X)$, of coherent sheaves. Let Γ be the set of D-brane charges, which is known to be given by topological K-theory [1]. The charge associated to a given object in the derived category is given by the map from the Grothendieck group of $\mathbf{D}(X)$ to Γ :

$$C : K(X) \rightarrow \Gamma. \tag{1}$$

Pick a candidate 0-brane charge $\gamma \in \Gamma$. The objects in $\mathbf{D}(X)$ corresponding to $C^{-1}(\gamma)$ are far too numerous to constitute the set of points of any target space X . This is illustrated, for example, by the well-known case of the flop [2]. Suppose X contains a rational curve C which may be flopped to produce a topologically distinct Calabi–Yau threefold X' containing the flopped curve C' . The derived categories $\mathbf{D}(X)$ and $\mathbf{D}(X')$ are equivalent. So $\mathbf{D}(X)$ contains objects corresponding to skyscraper sheaves on C' even though C' is not a curve in X .

The two-dimensional conformal field theory on the worldsheet does not allow all the objects in $\mathbf{D}(X)$ as D-branes. The D-branes that are truly physical must be Π -stable [3] (which, from now on, we refer to simply as “stable”). Unlike the derived category data, the stability condition depends on the complexified Kähler form $B + iJ \in H^2(X, \mathbb{C})$ which varies as one flops between X and X' . As is well-known, and we review in section 2, imposing stability eliminates just the right set of candidate 0-branes and the remaining set of D-branes nicely form a moduli space corresponding to the target space X , X' , or the singular space at the “middle” of the flop.

The purpose of this paper is to explore whether such a pretty picture exists for more subtle examples. The answer, we will see, is much less clear-cut. A general framework for providing numerous examples is given by the gauged linear sigma-model of [4]. In this context one has various phases one may probe by varying $B + iJ$. It is natural to ask if the geometry of other phases can be seen by D-brane probes.

The geometry of the other phases was previously explored by considering the complexified Kähler form $B + iJ$ itself. One may view this as measuring the areas of complex curves in X . In [5, 6] the value of $B + iJ$ was analytically continued using mirror symmetry from the large radius limit into other phases. The results for these linear sigma model examples suggest the following rules:

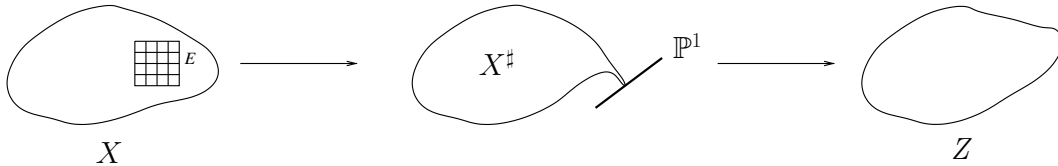


Figure 1: An exoflop extremal transition.

1. The smooth Calabi–Yau phases are as expected.
2. Geometric but singular phases such as orbifolds exhibit zero sizes in a limit. That is, if we move in the moduli space to blow an exceptional divisor down as far as possible while making the rest of the Calabi–Yau threefold infinitely large, we measure areas of curves in the exceptional set as zero. If X remains finite size, studied examples imply that it is impossible to shrink the exceptional divisors down to zero size.
3. Non-geometric phases containing Landau-Ginzburg theories or fibrations are pushed properly into the Kähler cone of a smooth phase. That is, no zero sizes are measured.

In the above analysis some choices of branch cuts need to be made to make these statements. We will discuss this further below. It was shown in [7] that an M-theory picture of measuring sizes gives the same result.

We will see in section 3.1 that the 0-brane probe picture of the orbifold coincides perfectly with the above. Indeed, the stability of the 0-brane is tied precisely to the value of $B + iJ$ in such a way that the exceptional set collapses to a point precisely when the corresponding component of J vanishes.

A much more interesting example concerns the “exoflop”. In this case, a phase change is achieved by shrinking down some divisor and then continuing (apparently) beyond the wall of the Kähler cone causing a \mathbb{P}^1 to protrude *outside* the Calabi–Yau threefold. The phase is considered non-geometric since this \mathbb{P}^1 has Landau–Ginzburg theory fibres over it. It is natural to ask if the 0-brane probe sees this \mathbb{P}^1 geometry. Another reason an exoflop example is of interest is that it is commonly associated to an extremal transition to a topologically distinct Calabi–Yau threefold Z . That is, when a smooth threefold X is exoflopped by shrinking down a divisor E , it typically becomes a union $X^\sharp \cup \mathbb{P}^1$, where X^\sharp is a singular threefold touching the external \mathbb{P}^1 at its singularity. The space X^\sharp then admits a deformation of complex structure resulting in a smooth space Z . We depict this process in figure 1. This exoflop extremal transition is the transition that connects the web of hypersurfaces in toric varieties as studied in [8].

An extremal transition is associated to massless D-branes as discussed in [9]. In the case of an exoflop, this actually happens in the exoflop *limit* rather than in the wall between phases. This leads to a conundrum. In the limit one might naïvely think that the \mathbb{P}^1 sticking out is very large but then it vanishes completely in the extremal transition.

We will resolve this somewhat by showing that the 0-brane doesn’t “see” the \mathbb{P}^1 and so the extremal transition makes more sense. Having said that, we will further show that, if

the threefold has finite volume, then the divisor E cannot be shrunk down to a point. Thus the extremal transition still seems very peculiar from the point of the view of the 0-brane moduli space. The geometry, as seen by the 0-brane, behaves discontinuously during the extremal transition as E jumps from nonzero size to not existing. As we discuss later, this paradox might be explained by considering string coupling effects.

Having failed to find the \mathbb{P}^1 of the exoflop we look at a simpler hybrid model in section 4. Here we find a candidate D-brane by using the technology of matrix factorizations. Its moduli space appears to be the \mathbb{P}^1 base of a Landau–Ginzburg fibration. It is interesting that this D-brane is only stable when one is close to the hybrid phase, i.e., it is unstable in the large radius limit. The charge of this D-brane is not that of a 0-brane. Therefore to probe the geometry of hybrid models we need to look further than 0-branes.

It should be emphasized that what one calls “the” geometry of a hybrid phase should be regarded as a pretty subjective statement. One can have different criteria for measuring the geometry. In this paper we see discrepancies between the geometry as seen by the critical points of the superpotential and the moduli space of 0-branes. There are other interesting ways of interpreting the geometry such as [10] (which has some overlap with section 4).

2 The Flop

In this section we review the well-known case of the flop as discussed in [2, 11, 12]. Let Y denote the singular conifold $xy = zw$ in \mathbb{C}^4 which may also be considered the quotient of \mathbb{C}^4 with coordinates (u_0, u_1, v_0, v_1) under the \mathbb{C}^* action $(u_0, u_1, v_0, v_1) \mapsto (\lambda u_0, \lambda u_1, \lambda^{-1} v_0, \lambda^{-1} v_1)$. Let $S = k[u_0, u_1, v_0, v_1]$ be the singly-graded homogeneous coordinate ring in the sense of Cox [13] with these weights. One may identify $x = u_0 v_0, y = u_1 v_1, z = u_0 v_1, w = u_1 v_0$.

Let X be a noncompact small resolution of the conifold given as the total space of the bundle $\mathcal{O}(-1) \oplus \mathcal{O}(-1)$ over \mathbb{P}^1 . The homogeneous coordinates of \mathbb{P}^1 are given by $[u_0, u_1]$ and the fibre directions are given by v_0 and v_1 . Let $C \cong \mathbb{P}^1$ denote the zero section, $v_0 = v_1 = 0$ of this bundle. There are numerous ways to deduce the result (essentially due to [14] and first manifesting itself in the physics literature in [15]) that $\mathbf{D}(X)$ is equivalent to the bounded derived category of finitely-generated representations of a quiver. Here we follow possibly the quickest way [16]. We find a tilting object

$$T = \mathcal{E}_0 \oplus \mathcal{E}_1 \oplus \dots \tag{2}$$

as a sum of line bundles in $\mathbf{D}(X)$. The endomorphism ring $\text{End}(T)$ is then the path algebra (with relations) of a quiver Q^{op} and $\mathbf{D}(X)$ is equivalent to the bounded derived category of finitely-generated representations of Q (with relations). We refer to [16] for details.¹ In our case, for the flop, we put

$$T = \mathcal{O} \oplus \mathcal{O}(1), \tag{3}$$

where $\mathcal{O}(n)$ is the sheaf associated to the S -module $S(n)$. If $\pi : X \rightarrow \mathbb{P}^1$ represents the fibration, then $\mathcal{O}(n)$ is the noncompactly supported sheaf $\pi^* \mathcal{O}_{\mathbb{P}^1}(n)$. Associating the node

¹Rather than use the opposite quiver, one can equivalently use *right* A -modules.

v_i to the summand $\mathcal{O}(i)$ in the tilting sheaf we obtain the quiver:

$$\begin{array}{ccc} & \begin{array}{c} v_0 \\ v_1 \end{array} & \\ \circ & \begin{array}{c} \curvearrowright \\ \curvearrowright \end{array} & \circ \\ v_0 & & v_1 \\ & \begin{array}{c} u_0 \\ u_1 \end{array} & \end{array} \quad (4)$$

with relations given by the superpotential $\text{Tr}(u_0 v_0 u_1 v_1 - u_0 v_1 u_1 v_0)$.

In general, let A be the opposite algebra of $\text{End}(T)$ and let e_i be the idempotent element of the path algebra given by zero length paths at node v_i . Then $P_i = Ae_i$ is the projective A -module given by all paths (with relations) starting at node v_i . The equivalence between $\mathbf{D}(X)$ and $\mathbf{D}(A\text{-mod})$ sends a summand \mathcal{E}_i of the tilting object to P_i .

Because X is a *noncompact* Calabi–Yau threefold, the K-theory class of a 0-brane in $\mathbf{D}(X)$ as we have described it is actually zero. Therefore we need to be careful about what we really mean by the “class” of a 0-brane. If we consider the derived category of *compactly supported* coherent sheaves on X then this is equivalent to the derived category of *finite-dimensional* quiver representations. See [17, 18] for a further discussion of this. Let V be a finite dimensional representation of the the quiver Q (or a complex of representations with this as the only nonzero entry). In the derived category of finite-dimensional representations of Q , the K-theory charge of V is simply given by its dimension vector (d_0, d_1, \dots) , where $d_i = \dim e_i V$. We will therefore use this as the characterization of being in the “class” of a 0-brane.

We will assume that the object in $\mathbf{D}(A\text{-mod})$ corresponding to a skyscraper sheaf is a complex with only one entry, i.e., it can be represented by a single quiver. This can be proven explicitly in each case we consider. Let V_p denote the quiver representation associated to a 0-brane, i.e., the skyscraper sheaf \mathcal{O}_p of a point and suppose it has dimension vector (d_0, d_1, \dots) . As was shown in [19],

$$\begin{aligned} \dim(\text{Hom}(P_i, V_p)) &= d_i \\ &= \dim(\text{Hom}(\mathcal{E}_i, \mathcal{O}_p)) \\ &= \text{rank}(\mathcal{E}_i) \\ &= 1. \end{aligned} \quad (5)$$

That is, the skyscraper sheaf corresponds to a quiver representation with dimension vector $(1, 1, \dots)$.

2.1 Moduli Space of Quiver Representations

In general the analysis of the moduli space of quiver representations can be fairly technical but has been studied in detail in, for example, [20, 21], and using dimer language [22, 23]. By viewing the quiver in terms of the endomorphism ring of a tilting object T we can find a very easy method that suffices for the examples in this paper. The idea of using tilting objects to compute the moduli space was discussed in detail in [24].

A quiver representation having the dimension vector $(1, 1, \dots)$ is specified by attaching a single number to each arrow. There is a class of isomorphisms acting within the set

of such representation by acting with an element of \mathbb{C}^* on each node. This leads to a torus action on the parameters associated to each arrow. The arrows on the quiver (4) are labeled by homogeneous coordinates from the identification with $\text{End}(T)$. (In general, the arrows will be associated with monomials in the homogeneous coordinates.) It is easy to see that the $(\mathbb{C}^*)^r$ action coming from the isomorphisms coincides with the toric $(\mathbb{C}^*)^r$ -action on the homogeneous coordinates. Furthermore, such labeling of the arrows in the quiver obviously satisfies any superpotential relationship since such constraints can be derived from the structure of $\text{End}(T)$ in the first place. *It is therefore natural to identify the homogeneous coordinates of the point p with the labels in the arrows of the quiver representation V_p .*

It is worth emphasizing this point as it is key to the constructions in the paper. The labels on the quiver (4) were first obtained from maps between the tilting summands given by multiplication by certain monomials in the homogeneous coordinates. But now we use these same labels for a quiver representation associated to a skyscraper sheaf of a point with these homogeneous coordinates. This parametrization of the skyscraper sheaves allows us to construct a moduli space naturally.

Of course, to construct a nice moduli space for our skyscraper sheaves we need to remove some affine subvariety before performing the $(\mathbb{C}^*)^r$ quotient on the homogeneous coordinates. The D-brane stability condition amounts to a θ -stability condition on the quiver in the sense of King [25] (as discussed in [26]) and so removes a suitable subvariety.

It should be emphasized that the general problem of constructing anything like a moduli “space” of stable objects is a subtle problem. To be rigorous one is forced into using the language of abstract stacks [27]. Even in the large radius limit it is difficult to prove that the set of 0-branes forms a nice moduli space [28]. Here we are able to use the language of quivers in all our examples to explicitly construct the moduli spaces in question.

We almost have a particularly cheap proof of the fact that the moduli space of 0-branes on a toric variety X is X itself. What we should really infer is that, for suitable stability conditions, X is a subspace of the moduli space of 0-branes. In general one can have multiple components of the moduli of 0-branes of which only one need be X . This happens, for example, for the case $\mathbb{C}^3/(\mathbb{Z}_2 \oplus \mathbb{Z}_2)$ as studied in [29]. In such cases, for the spurious extra components, one may parametrize the arrows in a way inconsistent with the labeling by homogeneous coordinates while still obeying the superpotential constraints. This does not happen for any example in this paper. For a more careful treatment we refer to [24].

2.2 The Moduli Space from Stability Conditions

Associating to zero the arrows labeled by v_0 and v_1 in the quiver (4) gives a representation of the Beilinson quiver for \mathbb{P}^1 [14]. This corresponds to D-branes supported on C . That is, objects in $i_*\mathbf{D}(\mathbb{P}^1)$ where $i : C \rightarrow X$ is the inclusion map. Accordingly, 0-branes lying on C will have $v_0 = v_1 = 0$.

Let (d_0, d_1) be the dimension vector of a representation of the quiver (4). The simple

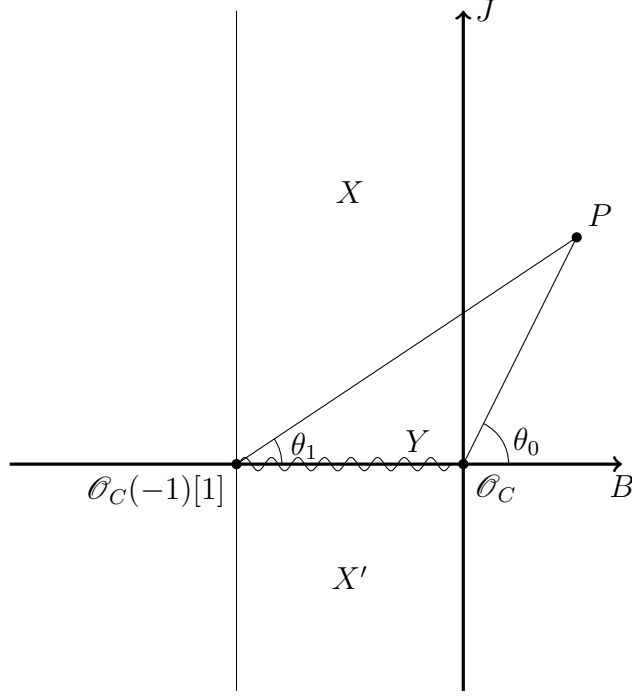


Figure 2: The $B + iJ$ plane for the flop.

one-dimensional representations have a correspondence:

$$\begin{aligned} (1, 0) &: \mathcal{O}_C \\ (0, 1) &: \mathcal{O}_C(-1)[1]. \end{aligned} \tag{6}$$

The complexified Kähler form in this noncompact Calabi–Yau space is parametrized by the complex number $\int_C(B + iJ)$. By abuse of notation we refer to this complex number as $B + iJ$. The central charge, Z , of the D-brane \mathcal{O}_C (and of any shift $\mathcal{O}_C[n]$) has a simple zero at the origin in the $B + iJ$ plane while $Z(\mathcal{O}_C(-1))$ has a simple zero at $B + iJ = -1$.

In figure 2 we show this $B + iJ$ plane with the above points labeled by their associated massless D-branes. Now consider the triangle

$$\begin{array}{ccc} \mathcal{O}_C(-1) & \xrightarrow{f} & \mathcal{O}_C \\ & \swarrow [1] & \searrow \\ & \mathcal{O}_p & \end{array} \tag{7}$$

where \mathcal{O}_p is the 0-brane, i.e., skyscraper sheaf associated to a point $p \in C$, the location of which is determined by the map f .

For Π -stability we associate a choice of “phase” of any object \mathcal{E} :

$$\xi(\mathcal{E}) = \frac{1}{\pi} \arg Z(\mathcal{E}), \tag{8}$$

(See [30] and references therein for a review.) With respect to this triangle, \mathcal{O}_p is stable if and only if

$$\xi(\mathcal{O}_C) - \xi(\mathcal{O}_C(-1)) = \frac{\theta_0 - \theta_1}{\pi} \leq 1. \quad (9)$$

In other words, \mathcal{O}_p decays as it passes below the line segment of the B -axis between the two massless D-brane points in figure 2.

Furthermore, if one does pass into the region of negative J by passing across this line segment, we have a triangle

$$\begin{array}{ccc} \mathcal{O}_C[-1] & \xrightarrow{g} & \mathcal{O}_C(-1)[1] \\ & \swarrow [1] & \searrow \\ & D_g & \end{array} \quad (10)$$

defining objects D_g which become stable. These new objects D_g can be interpreted as skyscraper sheaves of points on the *flopped* curve $C' \subset X'$ [2].

Note that *proving* an object is Π -stable is awkward as the logic is somewhat circular. The phases of objects in a distinguished triangle can only imply a decay of an object associated with one vertex of the triangle if the decay products themselves are stable. Now we know that \mathcal{O}_C is definitely stable where it becomes massless at $B + iJ = 0$ since it causes divergences in the 2-dimensional worldsheet field theory. Similarly $\mathcal{O}_C(-1)$ is most assuredly stable at the other massless D-brane point in figure 2. Thus, it does not seem too much of a leap of faith to assume that these two D-branes are both stable along the line segment joining these two points making our analysis is correct.

In this case one can rigorously prove these stability assertions by appealing to Bridgeland's definition of stability [31] (see also [32]). Here one reduces the stability statements to an *abelian* category given as the heart of a t-structure of $\mathbf{D}(X)$. This is most easily done when the phases of objects "line up" in a specific way. In our case, this abelian category \mathcal{A} is the category of representations of the quiver (4). Define a new phase

$$\phi(A) = \xi(A) + \frac{1}{2}, \quad (11)$$

so that $0 < \phi(A) < 1$ for all objects in \mathcal{A} so long as we remain between the lines $B = 0$ and $B = -1$ in figure 2. So long as we obey this condition, all stable D-branes are objects in \mathcal{A} (or their translates). An object A in \mathcal{A} is *semistable* so long as $\phi(E) \leq \phi(A)$ for any subobject $E \subset A$ and stable so long as $\phi(E) < \phi(A)$. The objects corresponding to \mathcal{O}_C and $\mathcal{O}_C(-1)[1]$ are then obviously stable as the dimension vector implies they have no nontrivial subobject.

Consider an object in \mathcal{A} with dimension vector (m, n) . This has phase

$$\phi(m, n) = \frac{1}{\pi} \arg i(nt + n - mt), \quad (12)$$

where $t = B + iJ$. Now the 0-brane \mathcal{O}_p , $p \in C$ is a quiver in the class $(1, 1)$ and is stable according to the following rules:

- If $(u_0, u_1) \neq (0, 0)$ and $(v_0, v_1) \neq (0, 0)$, \mathcal{O}_p has no subobject and is thus always stable.
- If $(u_0, u_1) = (0, 0)$ then $\mathcal{O}_C(-1)[1]$ is a subobject with dimension vector $(0, 1)$. This renders this 0-brane unstable if $\text{Im}(t) > 0$. So, if $J > 0$ we may regard $[u_0, u_1]$ as homogeneous coordinates giving the location of the 0-brane on C .
- If $(v_0, v_1) = (0, 0)$ then \mathcal{O}_C is a subobject with dimension vector $(1, 0)$. This renders this 0-brane unstable if $\text{Im}(t) < 0$. So, if $J < 0$ we may regard $[v_0, v_1]$ as homogeneous coordinates giving the location of the 0-brane on the flopped curve C' .

So far we have produced the expected moduli space of *stable* skyscraper sheaves when $J \neq 0$. Now consider the case where $\theta_1 - \theta_0 = \pi$, i.e., we lie on the line segment highlighted by the wiggly line in figure 2. Some quiver representations in the class $(1, 1)$ are now semistable with respect to decay into $(0, 1)$ and $(1, 0)$ but not strictly stable.

We claim one should use the notion of polystability. We will say that an object in $\mathbf{D}(X)$ is *polystable* if it is a direct sum of strictly stable objects (i.e., strict inequalities are used in stability conditions). This notion is copied from the study of Hermitian–Yang–Mills connections on vector bundles. A holomorphic vector bundle admits an Hermitian–Yang–Mills connection if and only if it is polystable [33, 34].

The reason why polystability is the correct notion for D-branes comes from the classical notion of mutually BPS solitons. It is well-known that there is no force between two BPS solitons. Thus, the combined classical state of two mutually BPS states is simply their direct sum.

A quiver representation with dimension vector $(1, 1)$ such that u_i are both zero or v_i are both zero is not strictly stable with respect to decay into $(0, 1) \oplus (1, 0)$. The only polystable object in this collection then consists of the direct sum where all four maps (u_0, u_1, v_0, v_1) are set to zero. That is, the origin of the conifold $x = y = z = w = 0$ is counted precisely once.

We have therefore shown that, when $\theta_1 - \theta_0 = \pi$, the moduli space of quivers with dimension vector $(1, 1)$ is the conifold Y . By using polystability, the moduli space of skyscraper sheaves yields X , X' or Y precisely, according to figure 2.

3 Shrinking Divisors

In this section we consider the case of varying $B + iJ$ so as to shrink a divisor E down to a point. Let's first give a very rough idea of how this differs from the flop case of the previous section.

Consider the short exact sequence

$$0 \longrightarrow \mathcal{I}_p \longrightarrow \mathcal{O}_E \longrightarrow \mathcal{O}_p \longrightarrow 0, \quad (13)$$

where \mathcal{O}_p is a 0-brane of a point $p \in E$ and \mathcal{I}_p is the ideal sheaf of p in E extended by zero. At large radius limit we know the phase of a sheaf \mathcal{E} is given by (see, for example, [30])

$$\xi(\mathcal{E}) = -\frac{1}{2} \dim \text{supp}(\mathcal{E}). \quad (14)$$

So $\xi(\mathcal{O}_E) = -1$ and $\xi(\mathcal{O}_p) = 0$. Now suppose, as is typical for Calabi–Yau threefolds from [35, 36], we have a point in the moduli space of conformal field theories where $Z(E)$ acquires a simple zero. Put this point at the origin of the $B + iJ$ moduli space as we did for the flop in figure 2. Now assume, again as is typical, that the phase $\xi(\mathcal{O}_E)$ remains constant as we follow the J -axis down from infinity. In order to destabilize a point \mathcal{O}_p via a decay associated to (13) the angle θ_0 in figure 2 would be expected to be $3\pi/2$ rather than the π seen for the flop (where the dimension of the support was only 1). It would appear that we get the 0-brane to decay by moving all the way to the limit of the phase in the lower half-plane of the figure. This gives a good picture of what actually happens. Rather than subspaces collapsing to a point on a phase *boundary* as happened for the flop, an exceptional divisor collapses at a phase *limit*.

3.1 An orbifold

The following is, in some sense, the simplest example of a compact Calabi–Yau threefold with an orbifold singularity. Let \mathcal{A} be a collection of 7 points in \mathbb{R}^5 with coordinates:

$$\begin{array}{c|ccccc}
 x_0 & 1 & 0 & 0 & 0 & 1 \\
 x_1 & 1 & 0 & 0 & 1 & 0 \\
 x_2 & 1 & 0 & 1 & 0 & 0 \\
 x_3 & 1 & 1 & 0 & 0 & 0 \\
 x_4 & 1 & -1 & -1 & -1 & -3 \\
 e & 1 & 0 & 0 & 0 & -1 \\
 p & 1 & 0 & 0 & 0 & 0
 \end{array} \tag{15}$$

Let Σ be a fan over a triangulation of this point set. We can associate a noncompact toric variety V_Σ in the usual way to this data. Let the homogeneous coordinates be named as in the left column of the table above. Now define a function on V_Σ :

$$W = p(x_0^2(x_1 + x_2 + x_3 + x_4) + e^2(x_1^7 + x_2^7 + x_3^7 + x_4^7)). \tag{16}$$

Let X_Σ be the critical point set of this function. Different triangulations of \mathcal{A} lead to different possibilities (or “phases”) for X_Σ . It is a simple matter to establish that there are four phases similar to the analysis in [37–39]

1. The orbifold phase: X_Σ is a hypersurface of degree 7 in the weighted projective space $\mathbb{P}_{\{3,1,1,1,1\}}^4$ with homogeneous coordinates $[x_0, \dots, x_4]$. There is an orbifold locally of the form $\mathbb{C}^3/\mathbb{Z}_3$ at $p = x_1 = \dots = x_4 = 0$.
2. The Calabi–Yau phase: The above orbifold point is blown up with an exceptional divisor $E \cong \mathbb{P}^2$ given by $p = e = 0$.
3. The Landau–Ginzburg phase: X_Σ is a fat point.
4. The hybrid phase: X_Σ is a fat \mathbb{P}^2 .

The convex hull of the point set \mathcal{A} is a reflexive polytope and we can construct the mirror following Batyrev [40]. The mirror to X_Σ is defined by a polynomial whose monomials naturally correspond to the homogeneous coordinates above via the monomial-divisor mirror map [41]. Let us denote the coefficients of these monomials by $\tilde{x}_0, \tilde{x}_1, \dots, \tilde{p}$. We can then form “algebraic coordinates” on the moduli space of theories:

$$\begin{aligned} y &= \frac{\tilde{x}_0 \tilde{e}}{\tilde{p}^2} \\ z &= -\frac{\tilde{x}_1 \tilde{x}_2 \tilde{x}_3 \tilde{x}_4}{\tilde{p} \tilde{e}^3}. \end{aligned} \quad (17)$$

In the smooth Calabi–Yau manifold we may define divisor classes H , corresponding to $x_1 = 0$, and L corresponding to $x_0 = 0$. It follows that $e = 0$ corresponds to the class $H - 3L$, and we have intersection numbers

$$H^3 = 63, \quad H^2L = 21, \quad HL^2 = 7, \quad L^3 = 2. \quad (18)$$

Let us write the complexified Kähler form as

$$B + iJ = hH + lL. \quad (19)$$

The monomial-divisor mirror map [41] (with sign corrections from [42]) then yields

$$\begin{aligned} h &= \frac{1}{2\pi i} \log(y) + O(y, z) \\ l &= \frac{1}{2\pi i} \log(z) + O(y, z), \end{aligned} \quad (20)$$

where $h(y, z)$ and $l(y, z)$ are uniquely determined from these asymptotics as ratios of solutions of the Picard–Fuchs equations $\square_z \Phi(y, z) = \square_y \Phi(y, z) = 0$, where

$$\begin{aligned} \square_z &= \left(z \frac{\partial}{\partial z} \right)^4 - \\ & z \left(1 + z \frac{\partial}{\partial z} + 2y \frac{\partial}{\partial y} \right) \left(y \frac{\partial}{\partial y} - 3z \frac{\partial}{\partial z} \right) \left(y \frac{\partial}{\partial y} - 3z \frac{\partial}{\partial z} - 1 \right) \left(y \frac{\partial}{\partial y} - 3z \frac{\partial}{\partial z} - 2 \right) \\ \square_y &= y \frac{\partial}{\partial y} \left(y \frac{\partial}{\partial y} - 3z \frac{\partial}{\partial z} \right) - y \left(2y \frac{\partial}{\partial y} + z \frac{\partial}{\partial z} + 1 \right) \left(2y \frac{\partial}{\partial y} + z \frac{\partial}{\partial z} + 2 \right). \end{aligned} \quad (21)$$

Consider first the limit of the moduli space when $y \rightarrow 0$, i.e., $\text{Im}(h) \rightarrow \infty$. This corresponds to the overall volume of the Calabi–Yau going to infinity. Let C be a line on E , the exceptional \mathbb{P}^2 . Then $[E]^2 = -3[C]$. It follows that

$$\int_C B + iJ = -\frac{1}{3}(hH + lL)(H - 3L)^2 = l. \quad (22)$$

So l , and thus z , controls the size of the blow-up. The limit $y \rightarrow 0$ decompactifies the Calabi–Yau threefold while keeping E finite.

Indeed, in this limit we have

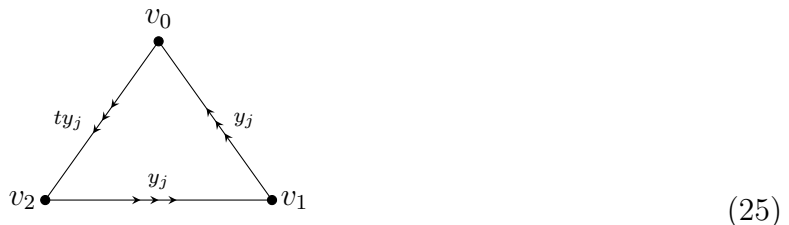
$$\square_z = \left(z \frac{\partial}{\partial z} \right) \square'_z, \quad (23)$$

where

$$\square'_z = \left(z \frac{\partial}{\partial z} \right)^3 + 27z \left(z \frac{\partial}{\partial z} \right) \left(z \frac{\partial}{\partial z} + \frac{1}{3} \right) \left(z \frac{\partial}{\partial z} + \frac{2}{3} \right). \quad (24)$$

which is familiar as the Picard–Fuchs equation for the blow-up of $\mathbb{C}^3/\mathbb{Z}_3$ [5]. For more details we refer to section 7.3 of [30].

In the noncompact limit $y \rightarrow 0$ let us model the geometry of $\mathbb{C}^3/\mathbb{Z}_3$ and its resolution torically. The resulting quiver description is very well-known [26]. Let the homogeneous coordinate ring be $S = k[t, y_0, y_1, y_2]$ with weights $(-3, 1, 1, 1)$. We use a tilting object $S \oplus S(1) \oplus S(2)$. This gives a quiver with three arrows between each node:



Let $\mathbf{D}(Q)$ be the derived category of finitely generated representations of the quiver (25) with relations which follow from the commutativity of the labeling of the arrows. Then $\mathbf{D}(Q)$ is a full subcategory of $\mathbf{D}(X)$. The quotient of $\mathbf{D}(X)$ by $\mathbf{D}(Q)$ corresponds to objects that are “pushed off to infinity” when we take the decompactification limit $y \rightarrow 0$. This can be seen by the fact that $\mathbf{D}(Q)$ gives a complete description of the local geometry of the blow-up of $\mathbb{C}^3/\mathbb{Z}_3$.

The situation now becomes fairly similar to the conifold in the previous section. Consider representations of this quiver with dimension vector (d_0, d_1, d_2) . As discussed in [26, 43], when we take the limit $z \rightarrow \infty$, corresponding to $l \rightarrow 0$, the phases, ξ , of all representations become equal. Thus we may describe all stable objects in an open neighbourhood of this limit by the abelian category of quiver representations. Setting $z = (3e^{-\pi i \psi})^{-3}$, we may draw lines of marginal stability in the ψ -plane,

The simple one-dimensional representations correspond to the so-called “fractional branes”: [26, 30]

$$\begin{aligned} (1, 0, 0) &: \mathcal{O}_E \\ (0, 1, 0) &: \Omega_E(1)[1] \\ (0, 0, 1) &: \mathcal{O}_E(-1)[2]. \end{aligned} \quad (26)$$

The skyscraper sheaves of a point, \mathcal{O}_p , have dimension vectors $(1, 1, 1)$. The stability of these objects was studied in detail in section 7.3.6 of [30]. If the point p lies on E then $t = 0$ which results some of the arrows in (25) being zero. This object is stable to decay against the subobjects $(1, 0, 0)$ and $(1, 1, 0)$ only if we lie in the grey region of figure 3 and the maps

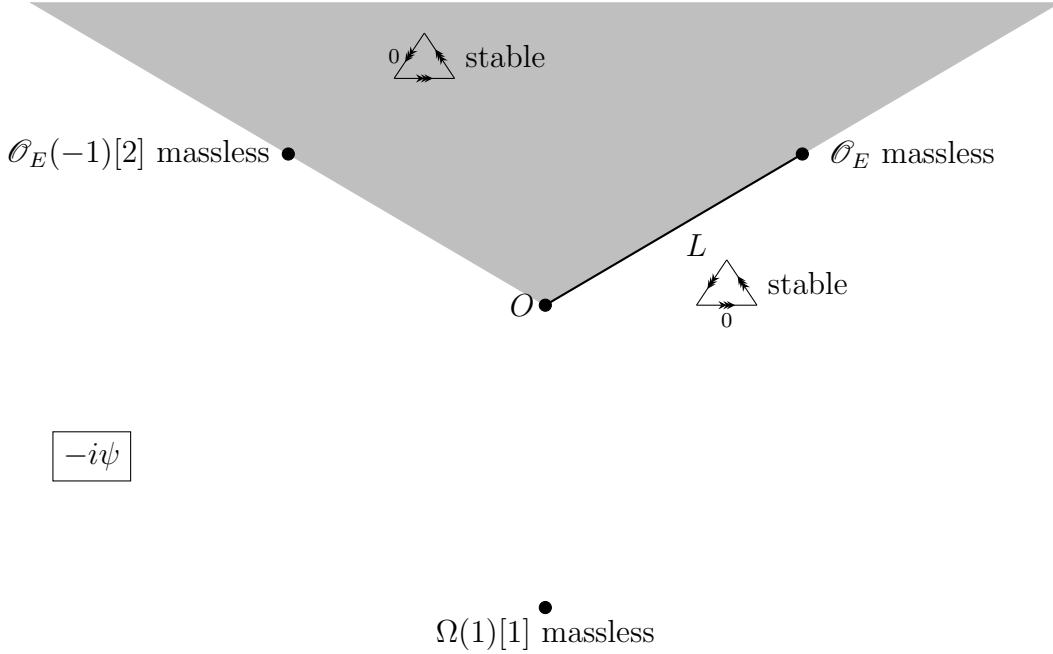


Figure 3: Regions of stability for objects with dimension vector $(1, 1, 1)$.

do not vanish on the other two sides of the triangle. The moduli space of these objects is \mathbb{P}^2 — in accordance with these being points on E .

Now consider the (interior of the) line labeled L in figure 3. \mathcal{O}_p becomes marginally stable against decay into the subobject of dimension $(1, 0, 0)$, i.e., \mathcal{O}_E . So, on L , \mathcal{O}_p becomes a polystable object $\mathcal{O}_E \oplus Q$, where Q is an object of dimension $(0, 1, 1)$. The maps between node v_1 and v_2 in Q cannot simultaneously vanish as that would destabilize it further. Thus, the moduli space of Q is still \mathbb{P}^2 . Therefore, *even though \mathcal{O}_p degenerates into a direct sum of stable objects along L , its moduli space remains the same.* When we pass beyond L , representations with maps between v_1 and v_2 set to zero become truly stable and still have moduli space \mathbb{P}^2 .

At the origin, O , when $\psi = 0$, if $t = 0$ then \mathcal{O}_p is only polystable as a direct sum of the three fractional branes. So, the exceptional divisor is replaced by a single point. This agrees with the picture that O corresponds to the orbifold point.

To summarize, we have proven the following for our noncompact resolution of $\mathbb{C}^3/\mathbb{Z}_3$, in precise agreement with what we would expect for our 0-brane probe:

Proposition 1 *In the neighbourhood of $\psi = 0$, where the stable objects always lie in the abelian category of representations of the quiver (25), the moduli space of objects with dimension vector $(1, 1, 1)$ is always the blown-up orbifold, except at $\psi = 0$, where it is the orbifold itself.*

Now let us try to analyze what happens when $y \neq 0$, i.e., we give our Calabi–Yau a finite volume. We immediately lose apparent contact with any quiver description of the complete category of D-branes. This is because the quiver picture arises from a *tilting object* in the derived category $\mathbf{D}(X)$. Serre duality for a compact manifold violates the tilting condition $\text{Hom}(T, T[n]) = 0$ for $n \neq 0$ and thus there is no hope of finding a tilting object. Indeed there is currently no known method of rigorously determining the complete stable spectrum of D-branes for any compact Calabi–Yau threefold.

Having said that, it seems reasonable to suppose that the possible decay modes of skyscraper sheaves should be unchanged between $y = 0$ and small values of y . In other words, the objects which were pushed off to infinity when $y \rightarrow 0$ are still far away in some sense. So, to determine whether \mathcal{O}_p is stable we can consider the same decay channels as above and we need only compute the change in phases, ξ , caused by a nonzero y . To phrase this another way, the quiver representations still provide a picture of a subcategory of $\mathbf{D}(X)$ and we restrict attention only to this subcategory.

As we saw above, the only issue to study is the question of whether all skyscraper sheaves \mathcal{O}_p , for $x \in E$, correspond to a single polystable object and thus E appears to collapse to a point. This happens when and only when the phases of the fractional branes become equal.

Let Φ_1 be the unique solution of the equations (21) which behaves as $1 + O(y, z)$ near the origin. This is $Z(\mathcal{O}_p)$, the central charge of the skyscraper sheaf. The central charges of the fractional branes can be determined as a solution of (21) by the method described in [44] which depends on the Chern characters of the objects in question. Let Φ_L be the unique solution that behaves as $\log(z)/2\pi i + O(z)$ and let Φ_{L^2} be the unique solution that behaves as $(\log(z)/2\pi i)^2 + O(z)$. The central charge of each fractional brane can be written as

$$a\Phi_1 + b\Phi_L + c\Phi_{L^2}, \tag{27}$$

for different real values of a, b, c . The only way the phases of all three fractional branes can align is if

$$\begin{aligned} \int_C J &= \text{Im}(l) \\ &= \text{Im} \frac{\Phi_L}{\Phi_1} \\ &= 0. \end{aligned} \tag{28}$$

Therefore, we have proven

Proposition 2 *The 0-brane probe condition for the divisor E to collapse to a point requires the classical condition that the area of C vanishes.*

This is exactly the problem studied in [6]. There it was shown in an example almost the same as this one that, for natural choices of branch cuts, when y is small and nonzero there is no choice of z that makes the area of X shrink to zero. The same is true here as we now show.

Putting $z = (3e^{-\pi i\psi})^{-3}$ and $y = -3\xi\psi$ we obtain good coordinates ξ, ψ in the neighbourhood of the orbifold limit point. One can show the periods have the following form near this limit point:

$$\begin{aligned}\Phi_1 &= 1 + \dots \\ \Phi_L &= \frac{2\pi\sqrt{3}}{\Gamma(\frac{2}{3})^3}\psi + \frac{63\Gamma(\frac{2}{3})^3}{\pi^2}\xi + \dots\end{aligned}\tag{29}$$

Following the logic of [6] we impose branch cuts to allow the above analytic continuation:

$$\begin{aligned}\frac{2\pi}{3} &< \arg(\psi) < \frac{4\pi}{3} \\ \frac{2\pi}{3} &< \arg(\xi) < \frac{4\pi}{3}\end{aligned}\tag{30}$$

If ξ is nonzero, that is we give a finite size to the Calabi–Yau threefold, we see that we cannot make the area of C vanish and thus the phases cannot align.

3.1.1 Discussion of branch cuts

It is certainly true that we may analytically continue the periods in such a way as to make components of $\text{Im}(J)$ vanish and thus align the periods to make it look as if some of the 0-branes decay. To do this we must venture past the branch cuts we imposed above. So what does this actually mean?

One can view the branch cuts as a boundary of a “fundamental” region for the moduli space. Every conformal field theory is accounted for by a point within this fundamental region. Going beyond the branch cuts we encounter points that are equivalent (as conformal field theories) to points in the fundamental region.

There is a close link between the idea of analytically continuing periods and monodromy as explained in [44]. Choose some basepoint in the moduli space of theories close to the large radius limit. Consider labeling B-type D-branes in a conformal field theory by associating them with specific objects in $\mathbf{D}(X)$. Now follow a path in the space of $B + iJ$ that extends beyond the branch cuts to some point P . There will be a point Q in the fundamental region which is equivalent to P if we apply an autoequivalence of $\mathbf{D}(X)$ to relabel the D-branes. A path from P to Q is a loop in the moduli space of theories. Monodromy around these loops results in the corresponding autoequivalence of $\mathbf{D}(X)$.

Thus, if we destabilize the 0-brane by going beyond the branch cuts, we can this as equivalent to destabilizing another D-brane while staying within the fundamental region. Thus, it is more natural to regard this as using another D-brane probe rather than the 0-brane.

The view we propose is that we fix a fundamental region by choosing cuts to make the 0-brane *as stable as possible*. This is the obvious choice if we want to retain the closest link to recognizable geometry. For the noncompact orbifold example above this still resulted in the 0-branes on E becoming unstable in the limit that E shrink to a point. For the compact

orbifold we were able to make the points of E always stable. By analytically continuing outside the fundamental region we discover that other D-branes may decay but they are not 0-branes — they are merely related to 0-branes by monodromy.

3.2 Shrinking a Quadric Surface

3.2.1 An exoflop extremal transition

Let \mathcal{A} be a collection of 8 points in \mathbb{R}^5 with coordinates:

$$\begin{array}{c|ccccc}
 p & 1 & 0 & 0 & 0 & 0 \\
 a & 1 & 1 & 0 & 0 & 0 \\
 b & 1 & 0 & 1 & 0 & 0 \\
 c & 1 & -2 & -1 & 0 & 0 \\
 d & 1 & 0 & 0 & 1 & 0 \\
 e & 1 & 0 & 0 & 0 & 1 \\
 f & 1 & -1 & 2 & -1 & -1 \\
 g & 1 & -1 & 0 & 0 & 0
 \end{array} \tag{31}$$

Let Σ be a fan over a triangulation of this point set. Again associate a noncompact toric variety V_Σ to this data. Let the homogeneous coordinates be named as in the left column of the table above. Now consider a lowest-order well-defined generic function on V_Σ which will be of the form (omitting coefficients)

$$W = p \left(a^2 + g^2 \left(b^4 (d^{10} + e^{10} + f^{10}) + c^4 (d^2 + e^2 + f^2) \right) \right) + \dots \tag{32}$$

Let X_Σ be the critical point set of this function. Again, different triangulations of \mathcal{A} lead to different phases for X_Σ . There are 10 distinct triangulations of \mathcal{A} but not all of these correspond to different phases of X_Σ . We are only concerned with two phases which we label by the corresponding Stanley–Reisner ideal I :

- The Calabi–Yau phase: $I = (bc, adef, g)$. X_Σ is a smooth threefold with $h^{1,1} = 2$ and $h^{2,1} = 144$ (courtesy of PALP [45]). Let X denote this manifold.
- The exoflop phase: $I = (pb, bc, acdef, g)$. The critical point set X_Σ is a reducible variety. One component is a threefold with an isolated singularity which we denote X^\sharp . The other component is a (fat) \mathbb{P}^1 which intersects X^\sharp transversely at its singular point. Such exoflops were first discussed in [39].

The convex hull of the points (31) is a reflexive polytope. If we delete the point corresponding to b , we change the convex hull but it is still reflexive. This latter polytope is associated to a Calabi–Yau threefold Z which is isomorphic to a resolved hypersurface of degree 10 in $\mathbb{P}^4_{\{5,2,1,1,1\}}$. It has Hodge numbers $h^{1,1} = 1$ and $h^{2,1} = 145$. If we deform the complex structure of Z so that the only monomials which appear in the defining equation correspond to those of (32) then Z becomes singular and isomorphic to X^\sharp .

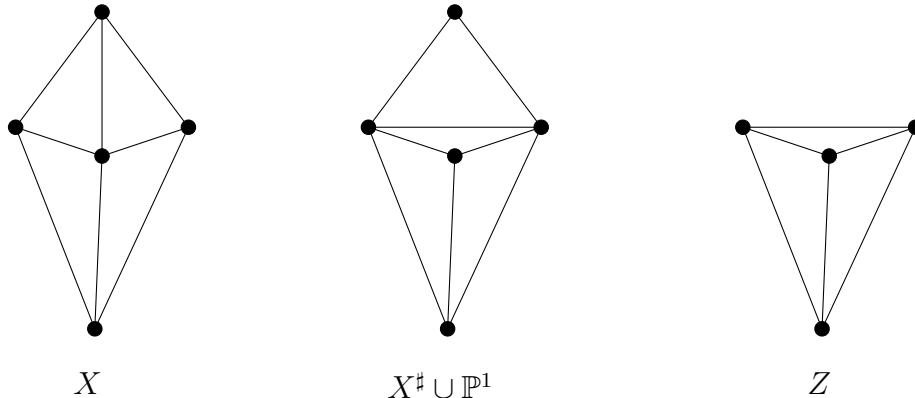


Figure 4: An extremal transition via an exoflop

The passage from X to Z via X^\sharp is an extremal transition exactly of the type discussed for connecting the web of Batyrev-like Calabi–Yau threefolds in [8]. The change in triangulation is shown schematically in figure 4. Note that this geometry shows that exoflops (rather than conifolds associated to regular flops) are the general mechanism for extremal transitions between hypersurfaces in toric varieties.

Suppose we are in the Calabi–Yau phase. The subvariety of V_Σ obtained by setting $p = b = 0$ is a \mathbb{P}^3 with homogeneous coordinates $[a, d, e, f]$. This intersects the Calabi–Yau X along the smooth quadric surface

$$a^2 + d^2 + e^2 + f^2 = 0, \quad (33)$$

which we denote E . In passing between the Calabi–Yau phase and the exoflop phase we shrink the \mathbb{P}^3 down in V_Σ and thus we shrink E down. Then, as the exoflop continues, a \mathbb{P}^1 grows out transverse to the Calabi–Yau threefold. At least, this is the geometric description according to the critical point set X_Σ . What we would like to know is whether the moduli space of skyscraper sheaves agrees with this. We will see that it does not.

A smooth quadric surface is always isomorphic to $\mathbb{P}^1 \times \mathbb{P}^1$. That said, when $\mathbb{P}^1 \times \mathbb{P}^1$ is embedded in \mathbb{P}^3 as a quadric surface, the homology classes of the two distinct rulings become equivalent. In other words, the two \mathbb{P}^1 families in the quadric have the same area. The fact that $h^{1,1}(X) = 2$ means that homology classes in X are all inherited from ones in the ambient toric variety. Thus, the two rulings of the quadric surface are homologous in X .

To describe the intrinsic geometry of E we will initially suppose the two rulings have different homology classes, but they will have to be equated once E is embedded in the Calabi–Yau threefold X .

3.2.2 The infinite volume case

As in the previous section, first let us make the approximation that all of the Calabi–Yau is large except for the quadric surface E . Thus, X looks like the canonical line bundle of

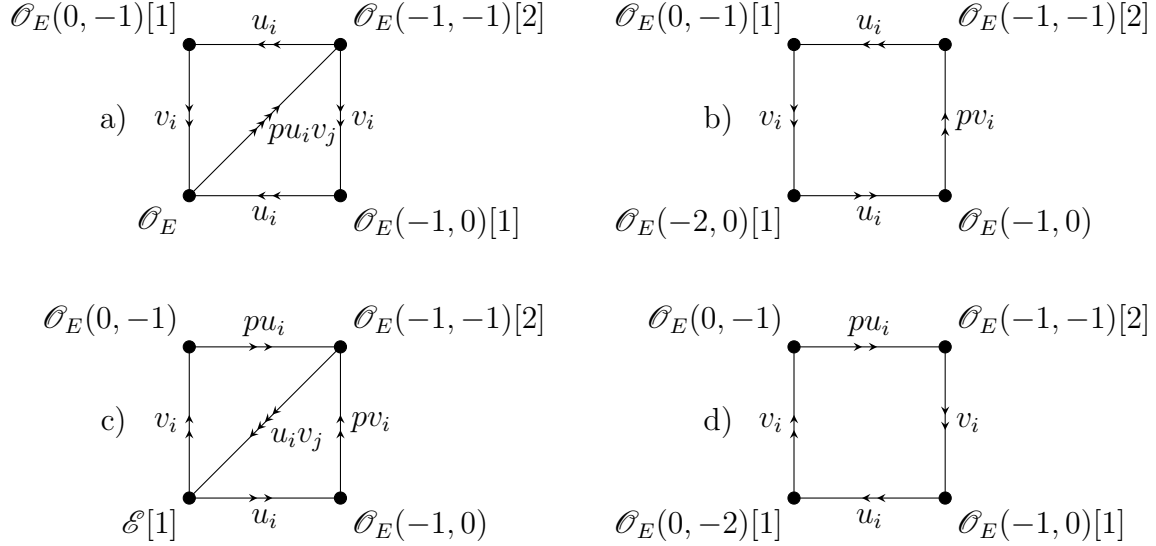


Figure 5: Quivers associated to a quadric surface.

the del Pezzo surface E . It is well-known [19, 29, 46, 47] how to analyze D-branes in this geometry using quivers.

Let $E \cong \mathbb{P}^1 \times \mathbb{P}^1$ have homogeneous coordinates $[u_0, u_1], [v_0, v_1]$ and let p denote the coordinate in the normal direction for the embedding of E in the Calabi–Yau threefold. Let $\mathcal{O}_E(m, n)$ denote a line bundle on E with first Chern class $me_1 + ne_2$ where e_1 is the 2-form dual to one of the rulings by \mathbb{P}^1 and e_2 is dual to the other. In our noncompact limit we have a fibration $\pi : X \rightarrow E$. Let $\mathcal{O}(m, n)$ denote $\pi^* \mathcal{O}_E(m, n)$. To describe $\mathbf{D}(X)$ we need a tilting collection which amounts to much the same thing as asking for an exceptional collection on E . One can find tilting collections of line bundles for a toric example such as this one by using the method described in [16]. There are four choices of interest:

- a) $\mathcal{O} \oplus \mathcal{O}(0, 1) \oplus \mathcal{O}(1, 0) \oplus \mathcal{O}(1, 1)$
- b) $\mathcal{O} \oplus \mathcal{O}(0, 1) \oplus \mathcal{O}(-1, 0) \oplus \mathcal{O}(1, 1)$
- c) $\mathcal{O} \oplus \mathcal{O}(0, -1) \oplus \mathcal{O}(-1, 0) \oplus \mathcal{O}(1, 1)$
- d) $\mathcal{O} \oplus \mathcal{O}(0, -1) \oplus \mathcal{O}(1, 0) \oplus \mathcal{O}(1, 1)$

These are all related by a tilting equivalence which is a form of Seiberg duality [48].

The corresponding quivers are shown in figure 5. Associated to each node in the quiver is an object (a “fractional brane”) corresponding to a dimension one representation of the quiver. We label each vertex in figure 5 by the corresponding fractional brane. A straightforward method for determining these fractional branes comes from [16]. The sheaf \mathcal{E} in figure

5c) corresponds to a rank 3 vector bundle on E and is given by the short exact sequence

$$0 \longrightarrow \mathcal{O}_E(-2, -2) \xrightarrow{\begin{pmatrix} u_0 v_0 \\ u_1 v_0 \\ u_1 v_1 \end{pmatrix}} \mathcal{O}_E(-1, -1)^{\oplus 4} \longrightarrow \mathcal{E} \longrightarrow 0. \quad (34)$$

The maps along the edges of the quiver label the corresponding homomorphisms between the summands of the tilting collection (with the arrows reversed) and, as above, these labels will also be associated to the homogeneous coordinates of the location of a 0-brane. The quiver relations coming from the superpotential can easily be read off from this labeling simply from the fact that the coordinates u_i, v_i, p commute.

The analysis of the Picard-Fuchs equation for this system was performed in [19]. Let $B + iJ = t_1 e_1 + t_2 e_2$. On the mirror, we have B-model algebraic coordinates z_1, z_2 such that

$$\begin{aligned} t_1 &= \frac{1}{2\pi i} \log(z_1) + O(z_1, z_2) \\ t_2 &= \frac{1}{2\pi i} \log(z_2) + O(z_1, z_2). \end{aligned} \quad (35)$$

Let us also use the notation t_{12} for the period which asymptotically goes as

$$t_{12} = t_1 t_2 + O(z_1, z_2). \quad (36)$$

There are four linearly independent solutions of the Picard–Fuchs equation corresponding to the even cohomology of E . By using the techniques of [5, 6] we find the following solutions:

$$\begin{aligned} \Phi_0(z_1, z_2) &= 1 \\ \Phi_1(z_1, z_2) &= t_1 - \frac{1}{2} = \frac{1}{2\pi i} \log(e^{-i\pi} z_1) + \frac{1}{i\pi} \sum_{(m,n) \neq (0,0)} A_{mn} z_1^m z_2^n \\ \Phi_2(z_1, z_2) &= t_2 - \frac{1}{2} = \frac{1}{2\pi i} \log(e^{-i\pi} z_2) + \frac{1}{i\pi} \sum_{(m,n) \neq (0,0)} A_{mn} z_1^m z_2^n \\ \Phi_3(z_1, z_2) &= t_{12} - \frac{1}{2}(t_1 + t_2) + \frac{1}{4} = -\frac{1}{4\pi^2} \left(\log(e^{-i\pi} z_1) \log(e^{-i\pi} z_2) \right. \\ &\quad \left. + \sum_{(m,n) \neq (0,0)} A_{mn} z_1^m z_2^n (\log(e^{-i\pi} z_1) + \log(e^{-i\pi} z_2) + \chi_{mn}) \right) \end{aligned} \quad (37)$$

where

$$\begin{aligned} A_{mn} &= \frac{\Gamma(2m + 2n)}{\Gamma(m + 1)^2 \Gamma(n + 1)^2}, \\ \chi_{mn} &= 4\Psi(2m + 2n) - 2\Psi(m + 1) - 2\Psi(n + 1), \end{aligned}$$

and $\Psi(z)$ is the usual di-Gamma function, and the sum $\sum_{(m,n) \neq (0,0)}$ runs over all non-negative m, n with the exception of $m = n = 0$. The power series converge for $|z_1| < \frac{1}{4}$ and $|z_2| < \frac{1}{4}$

which corresponds to the large radius limit phase. We may analytically continue beyond this phase to obtain the following, where $y_1 = z_2^{-1}z_1$ and $y_2 = z_2^{-1}$:

$$\begin{aligned}
\Phi_0(y_1, y_2) &= 1 \\
\Phi_1(y_1, y_2) &= \frac{1}{2\pi i} \log(y_1) + \Phi_2(y_1, y_2) \\
\Phi_2(y_1, y_2) &= -\frac{1}{2\pi i} (e^{i\pi} y_2)^{\frac{1}{2}} \sum_{m,n \geq 0} B_{mn} y_1^m y_2^n \\
\Phi_3(y_1, y_2) &= \frac{1}{12} - \frac{1}{4\pi^2} (e^{i\pi} y_2)^{\frac{1}{2}} \sum_{m,n \geq 0} B_{mn} y_1^m y_2^n (-\log(y_1) + \tilde{\chi}_{mn}),
\end{aligned} \tag{38}$$

where expressions for B_{mn} and $\tilde{\chi}_{mn}$ can be found in [19].

When this del Pezzo surface is embedded into the Calabi–Yau threefold we must set $z_1 = z_2$. This puts us right on the limit of convergence for the power series in (38). The limit of the exoflop phase corresponds to $y_1 = 1$ and $y_2 = 0$. That is, $\Phi_0 = 1$, $\Phi_1 = \Phi_2 = 0$ and $\Phi_3 = 1/12$. This, in turn implies $t_1 = t_2 = 1/2$ and $t_{12} = 1/3$.

The fact that $t_1 = t_2 = 1/2$ in this limit implies that the Kähler form J is zero and B has component $1/2$ on each ruling. So, using the criteria of [5], by measuring areas with the Kähler form, E has shrunk down to zero size. Is the same true using the moduli space of 0-branes?

The central charges of interest are given by

$$Z(\mathcal{O}_E(-m, -n)) = \left(\frac{7}{6} - m - n + mn\right) + (n-1)t_1 + (m-1)t_2 + t_{12}, \tag{39}$$

which gives

$$Z(\mathcal{O}_E(-m, -n)) = \frac{1}{2} + mn - \frac{1}{2}(m+n) \tag{40}$$

in the exoflop limit. In particular, we have

$$Z(\mathcal{O}_E(-1, 0)) = Z(\mathcal{O}_E(0, -1)) = 0, \tag{41}$$

giving two massless fractional D-branes in each of the quivers in figure 5. In each case the other two fractional branes have central charge equal to $1/2$.

When we embed E into X we identify the classes e_1 and e_2 , and thus $\mathcal{O}_E(-1, 0)$ and $\mathcal{O}_E(0, -1)$ have the same Chern class. That said, they are two distinct objects in the derived category and thus two distinct D-branes. To see this, note that $\text{Hom}(\mathcal{O}_E(-1, 0), \mathcal{O}_E(0, -1)) = 0$.

Stable massless D-branes correspond to singular conformal field theories and, indeed, one can compute the discriminant

$$\Delta = 16y_1^2 - 8y_1y_2 + y_2^2 - 32y_1 - 8y_2 + 16, \tag{42}$$

to confirm that $y_1 = 1, y_2 = 0$ is singular.

The fact that *two* D-branes become massless means that we have an extremal transition, following [9]. Indeed, it is precisely two massless states that are required to change the Hodge numbers from $(2, 144)$ to $(1, 145)$.

One should note that the point in moduli space where $z_1 = z_2 = 1/4$ is also of interest. This is where the discriminant intersects the wall between the Calabi–Yau phase and the exoflop phase. In this case just a single D-brane goes massless according to the EZ analysis of [35, 36]. Hence there is no extremal transition here; just a singular conformal field theory. It is worth emphasizing that this exoflop example is a little unusual compared to simpler examples in that the limit point of the phase, and not just the phase transition wall, hits the discriminant.

The quiver associated to the exoflop limit is the one where all the phases of the simple objects align. Typically this picks out a unique quiver. This is because tilting transformations of the type studied in [19] replace one of the fractional branes by an anti-brane which therefore destroys any alignment of phases. The exception to this, of course, is when certain fractional branes are massless. Then the tilted quiver replacing a brane by its anti-brane is just as valid. In our case all four quivers listed in figure 5 are relevant.

The quiver representation associated to the 0-brane has dimension vector $(1, 1, 1, 1)$ in all four cases and the labels on the edges correspond to the required maps in the representation to move the 0-brane around X . Thus, to place the 0-brane on E we set any edge containing a p to zero. The quiver c) in figure 5 is of particular interest in this case. For 0-branes on E we have a short exact sequence

$$0 \longrightarrow \begin{array}{ccc} 0 & \longrightarrow & 1 \\ \uparrow & \nearrow & \uparrow \\ 1 & \longrightarrow & 1 \end{array} \longrightarrow \begin{array}{ccc} 1 & \longrightarrow & 1 \\ \uparrow & \nearrow & \uparrow \\ 1 & \longrightarrow & 1 \end{array} \longrightarrow \begin{array}{ccc} 1 & \longrightarrow & 0 \\ \uparrow & \nearrow & \uparrow \\ 0 & \longrightarrow & 0 \end{array} \longrightarrow 0. \quad (43)$$

This shows how the fractional brane $\mathcal{O}_E(0, -1)$ can break off the 0-brane. Similar $\mathcal{O}_E(-1, 0)$ can also be a decay product. Now both of these fractional branes are massless at the exoflop point and have no well-defined phase $\arg(Z)$. The obvious treatment of this case, using the usual BPS mass rules, is to assert that the 0-brane is marginally stable against decays involving these decay products. A rigorous argument along these lines is a little delicate because we are assuming we are in a classical zero-string coupling limit. In fact, the actual D-brane mass is proportional to Z/g , where g is the string coupling and so all of our D-branes are really infinitely massive except for the ones that are suddenly massless when $Z = 0$.

From now we will assume that massless decay products lead to marginal stability. When we see unexpected results for the moduli spaces later on this paper it should be noted that things cannot be improved by changing the rules for the treatment of these massless D-branes.

Anyway, what remains after the two massless branes $\mathcal{O}_E(0, -1)$ and $\mathcal{O}_E(-1, 0)$ break off is a marginally bound state of $\mathcal{E}[1]$ and $\mathcal{O}_E(-1, -1)[2]$. Thus, as in the orbifold case, the 0-brane decays into a direct sum of fractional branes and this is the only polystable state.

So, at the exoflop limit point, the ruled surface E has been replaced by a point. This situation is similar to the orbifold of section 3.1. Note, in particular that the 0-branes do

not see the exoflop geometry. There is no deformation of the 0-brane on the collapsed E which could be interpreted as moving into the external \mathbb{P}^1 . The only deformation of the direct sum of the 4 fractional branes consists of switching p on which corresponds to moving away from E into the bulk of X . This can be proven by noting that the quivers we consider can be interpreted as “Ext-quivers”, where the arrows denote Ext^1 's between the simple one-dimensional representations. Any deformation within the category of quiver representations of a direct sum of simple objects will be given, to first order, by an extension. Thus we really can only deform a D-brane by changing the values associated to the arrows.

One explanation for the loss of the exoflopped \mathbb{P}^1 is as follows. In order to see the \mathbb{P}^1 sticking out of the Calabi–Yau threefold we would need to move in the Kähler moduli space *beyond* the stage where E collapses to a point as in the flop case of section 2. Here, E collapses to a point just as we hit the limit point in the moduli space and there is nowhere further to go. Actually we may well be able to “see” the \mathbb{P}^1 using different D-brane probes as will become apparent in section 4.

3.2.3 The finite volume case

Now consider what happens when we give X finite size. The situation is very similar to the orbifold of section 3.1 in that it now becomes impossible to shrink E to a point. In particular, let us try to follow the discriminant locus where $\mathcal{O}_E(-1, 0)$ and $\mathcal{O}_E(0, -1)$ are massless as X acquires finite size. Introduce coordinates on the moduli space

$$z = y^{-1} = \frac{\tilde{a}\tilde{d}\tilde{e}\tilde{f}}{\tilde{p}^2\tilde{b}^2}, \quad w = \frac{\tilde{a}^2\tilde{b}\tilde{c}}{\tilde{p}^4}. \quad (44)$$

The coordinate w controls the overall size of the Calabi–Yau threefold X with $w = 0$ being the large radius limit. The coordinate z (and thus y) coincides with the same coordinate in the previous subsection when $w = 0$. We want to allow w to become small but nonzero.

The discriminant can be computed as

$$\Delta = 12800000w^2 - 262144y^2w^3 - 1024000yw^2 + 12288y^2w^2 + 3200yw - 192y^2w - 16y + y^2. \quad (45)$$

We know that two D-branes become massless for solutions of this equation near $(y, w) = (0, 0)$ as this is where the extremal transition occurs and we know from above that these must be $\mathcal{O}_E(-1, 0)$ and $\mathcal{O}_E(0, -1)$ (using the notation from the previous section).

As w is switched on, the expression for the central charges (39) needs to be reinterpreted a little. The constant 1 is no longer an exact period and t_1 is forced equal to t_2 . We write the three independent periods in question as t^0 , t and t^2 , and (39) becomes

$$Z(\mathcal{O}_E(-m, -n)) = \left(\frac{7}{6} - m - n + mn\right)t^0 + (n + m - 2)t + t^2, \quad (46)$$

To stay on the discriminant we require

$$Z(\mathcal{O}_E(-1, 0)) = \frac{1}{6}t^0 - t + t^2 = 0, \quad (47)$$

i.e., set $t^2 = t - \frac{1}{6}t^0$. Given any small w we know that we can fix y such that we stay on the discriminant in this fashion. This is because the extremal transition can be made to occur for any large but finite volume of the Calabi–Yau threefold.

Quiver c) in figure 5 will again be the important one. We have

$$\begin{aligned} Z(\mathcal{O}_E(-1, -1)[2]) &= t \\ Z(\mathcal{E}[1]) &= t^0 - t. \end{aligned} \tag{48}$$

When w is switched on and kept away from branch cuts, an analysis very similar to section 3 and [6] shows that the component of the Kähler form that measures the areas of the rulings in E becomes strictly positive. The mirror map dictates that the relevant component of $B + iJ$ is given by the ratio of periods t/t^0 . That is,

$$\text{Im}(t/t^0) > 0. \tag{49}$$

We know that the phases of the central charges $\xi(\mathcal{O}_E(-1, -1)[2])$ and $\xi(\mathcal{E}[1])$ are equal when $z = w = 0$ since that corresponds to a contracted del Pezzo surface.² It follows that they are almost equal when w is small and thus (49) gives

$$\xi(\mathcal{O}_E(-1, -1)[2]) > \xi(\mathcal{E}[1]). \tag{50}$$

This means that $\mathcal{O}_E(-1, -1)[2]$ and $\mathcal{E}[1]$ can form a stable bound state $\mathcal{G}(f)$ from the triangle

$$\begin{array}{ccc} \mathcal{O}_E(-1, -1)[2] & \xrightarrow{[1] f} & \mathcal{E}[1] \\ & \searrow & \swarrow \\ & \mathcal{G}(f) & \end{array} \tag{51}$$

where f comes from the diagonal map in figure 5c). That is, f is any linear combination of $u_0v_0, u_0v_1, u_1v_0, v_0v_1$. The moduli space of objects $\mathcal{G}(f)$ is therefore $\mathbb{P}^1 \times \mathbb{P}^1$, i.e., E .

So, to recap, when we lie on the discriminant locus for small values of y and w and we consider a 0-brane on the quadric surface E , this D-brane becomes marginally stable against a decay into two massless D-branes and $\mathcal{G}(f)$. We have a polystable D-brane

$$\mathcal{O}(0, -1) \oplus \mathcal{O}(-1, 0) \oplus \mathcal{G}(f). \tag{52}$$

But the moduli space of such polystable D-branes is the moduli space of $\mathcal{G}(f)$ which is precisely E . So our 0-brane probe says that E has *not* shrunk down to a point.

In one sense this is an expected result. The criterion for when E has shrunk down by measuring areas says that it cannot when X has finite volume. So the 0-brane probe picture agrees. That said, in another sense this is a very surprising result. When the two D-branes become massless as we hit the discriminant we have an extremal transition to another

²It is believed this a general result and can be proven for contracted exceptional sets in orbifolds [43]. In this case the quadric surface can be obtained from a partial resolution of an orbifold, as in [29], and thus the result is proven.

Calabi–Yau threefold Z . From Z 's point of view, the extremal transition occurs because of a singularity induced by a deformation of complex structure. For a large generic value of the Kähler form, the moduli space of a 0-brane on Z is simply Z . So, from Z 's point of view the 0-brane probe says that E has shrunk to a point at the moment the extremal transition happens. But from X 's point of view it has not. In the extremal transition the volume of E appears to jump discontinuously from some nonzero size to zero.

A resolution of this apparent paradox might come from the fact that we have not considered the effects of a nonzero string coupling. The idea that D-branes have a moduli space is a strictly conformal (or topological) field theory notion for zero string coupling. Once the string coupling is turned on we need to quantize the D-branes and, if the moduli space is reasonably well-defined, for the ground states this amounts to computing the cohomology of the moduli space. The resulting spectrum of D-branes can certainly jump as we move around the moduli space of theories. This happens all the time in wall-crossing phenomena such as [49] and there are no paradoxes here. Matters become a good deal more complicated when non-ground-states for the D-branes are considered. The notion of a location of a 0-brane is contained in the complete string theory. But this is very difficult to analyze so we will not try to pursue this here.

Let us emphasize that the peculiar behaviour arising from the impossibility of shrinking E down does not arise from our rules for treating massless D-branes. The moduli space of the polystable D-brane (52) arises from the moduli space of the massive part $\mathcal{G}(f)$. Whether we keep the massless parts bound or not will not collapse the moduli space down to a point.

4 Probing a Hybrid \mathbb{P}^1

4.1 Basic geometry

In the previous section we failed to “see” the \mathbb{P}^1 sticking out of the Calabi–Yau threefold in an exoflop phase. Recall that this \mathbb{P}^1 is actually a hybrid model in the sense that there is a Landau–Ginzburg (orbifold) theory over every point in the \mathbb{P}^1 . It is natural to ask whether a D-brane probe can ever see the geometry of such a hybrid phase. That is, can we find a D-brane whose moduli space is \mathbb{P}^1 ?³

One easy way to obtain a hybrid model is to consider a Calabi–Yau threefold X that has a fibration $\pi : X \rightarrow \mathbb{P}^1$ with generic fibre a K3 surface. Assume for simplicity that this fibration has a section $C \subset X$. If we vary the Kähler form to shrink down X while keeping C constant we will generically pass into a hybrid model of the desired type. Each K3 fibre will become a Landau–Ginzburg theory. Imagine a 4-brane corresponding to \mathcal{O}_S where S is a generic K3 fibre. The moduli space of such a brane should indeed be \mathbb{P}^1 . But this is not a very impressive result — we have not really probed anything about the hybrid phase since our result has an interpretation purely in terms of the geometry of the Calabi–Yau phase.

Instead we could look at an example where the \mathbb{P}^1 has no geometric manifestation in the Calabi–Yau phase. To this end let X be a complete intersection of two generic cubic

³Perhaps if we were more ambitious we could try to find a *fat* \mathbb{P}^1 but we will not discuss this here.

equations in \mathbb{P}^5 . The toric geometry used to deal with complete intersections is inherent in Witten’s original phases work [4] and was described further in [50, 51]. \mathcal{A} is a collection of 8 points in \mathbb{R}^7 :

$$\begin{array}{l|ccccccc}
p_0 & 0 & 1 & 0 & 0 & 0 & 0 & 0 \\
p_1 & 1 & 0 & 0 & 0 & 0 & 0 & 0 \\
x_0 & 0 & 1 & 1 & 0 & 0 & 0 & 0 \\
x_1 & 0 & 1 & 0 & 1 & 0 & 0 & 0 \\
x_2 & 0 & 1 & 0 & 0 & 1 & 0 & 0 \\
x_3 & 1 & 0 & 0 & 0 & 0 & 1 & 0 \\
x_4 & 1 & 0 & 0 & 0 & 0 & 0 & 1 \\
x_5 & 1 & 0 & -1 & -1 & -1 & -1 & -1
\end{array} \tag{53}$$

A triangulation of this point set defines a noncompact Calabi–Yau toric variety V_Σ . Define the worldsheet superpotential

$$W = p_0 f_0 + p_1 f_1, \tag{54}$$

which is an invariant function on V_Σ , where f_0 and f_1 are cubic polynomials in x_0, \dots, x_5 . Again we define X_Σ as the critical point set of W : There are two triangulations of \mathcal{A} leading to two phases. We label them by B_Σ , the Alexander dual of the Stanley-Reisner ideal I_Σ (which is the ideal associated to the variety removed from affine space prior to quotienting to form the toric variety).

- The Calabi–Yau phase: $B_\Sigma = (x_0, x_1, x_2, x_3, x_4, x_5)$. X_Σ is a smooth threefold given by the complete intersection of two cubics in \mathbb{P}^5 . The \mathbb{P}^5 has homogeneous coordinates $[x_0, \dots, x_5]$.
- The hybrid phase: $B_\Sigma = (p_0, p_1)$. X_Σ is a (fat) \mathbb{P}^1 with homogeneous coordinates $[p_0, p_1]$. Over each point in this \mathbb{P}^1 there is a cubic Landau-Ginzburg orbifold theory with fields x_0, \dots, x_5 .

If life were the same as the flop we would have a 0-brane moduli space of a Calabi–Yau threefold in the Calabi–Yau phase and a 0-brane moduli space of \mathbb{P}^1 in the hybrid phase. This is not at all what happens. Applying the discussion at the start of section 3, it is even harder to destabilize the zero brane since we are shrink down the *entire* 3-dimensional Calabi–Yau when passing to the hybrid phase. Naïvely we might expect the angle θ_0 in figure 2 to be 2π . This implies that the 0-brane fails to decay even in the limit of the hybrid. This is the analogue of the statement that the 0-brane is stable for the Gepner model of the quintic for which evidence has been given in [52, 53].

So it would seem that the moduli space of 0-branes is *always* the Calabi–Yau threefold irrespective of where we are in the moduli space. However, from the hybrid’s point of view we are only shrinking down a curve when moving out of its phase and so we would expect life to be similar to the flop. That is, the geometry-probing D-brane should be stable only in the hybrid phase. We should therefore expect *two* different classes of D-branes — the 0-brane which always gives the Calabi–Yau picture and another probe that gives the \mathbb{P}^1 picture only in the hybrid phase. This is exactly what we find below.

4.2 Equivalences between D-branes between the 2 phases

The mathematical machinery required to understand D-branes for complete intersections in toric varieties is based on matrix factorizations [54] and was discussed in [55–57]. The first question we wish to address is how to identify D-branes in one phase with D-branes in the other. In particular, we need the large Calabi–Yau interpretation of a certain D-brane in the hybrid phase.

We begin with a tilting object for V_Σ . Let S be the homogeneous coordinate ring $k[p_0, p_1, x_0, \dots, x_5]$. Let

$$T = S \oplus S(-1) \oplus \dots \oplus S(-5). \quad (55)$$

This is a tilting object for V_Σ in both phases.

Now add a second grading to the picture which is associated to the $U(1)$ R -charge of the gauged linear sigma model. Let p_0 and p_1 have bigrading $(2, -3)$ and x_0, \dots, x_5 have bigrading $(0, 1)$. So W has grade $(2, 0)$ as one would expect for the worldsheet superpotential.

Following [55, 56] we define the category of matrix factorizations of W :

$$\mathrm{DGrS}(W) = \frac{\mathbf{D}(\mathrm{gr}\text{-}S')}{\mathfrak{P}\mathrm{erf}(S')} \Big|_{[1]=(1,0)}. \quad (56)$$

where $S' = S/(W)$ and $\mathfrak{P}\mathrm{erf}(S')$ is the triangulated subcategory of $\mathbf{D}(\mathrm{gr}\text{-}S')$ given by objects with a *finite* free resolution. We refer to [55] for a careful treatment of the boundedness of the various derived categories involved.

The subscript in (56) refers to the fact that we must identify the homological grading with the R -charge. That is, in the triangulated category $\mathrm{DGrS}(W)$ we identify the translation functor $[1]$ with the grading shift $(1, 0)$. Because of this identification we will rewrite $S(a, b)$ as $S(b)[a]$ when we give explicit matrix factorizations.

In practice, the mapping between S' -modules and matrix factorizations given by the equivalence (56) is quite easy to obtain. Given an S' -module M compute a minimal free resolution. This resolution will be infinite but asymptotically cyclic of period 2 as discovered by Eisenbud [58]. The matrix factorization can be read off from this asymptotic form.

The category of D-branes in the phase associated to a triangulation Σ is then the quotient of $\mathrm{DGrS}(W)$ by T_Σ^Δ , where T_Σ^Δ is the sub-triangulated category of matrix factorizations generated by modules annihilated by powers of B_Σ [57]. Of course, it is a basic property of topological B-type D-branes that they should not depend on Σ .

There is an equivalence of categories [56, 58–60]

$$\mathrm{DGrS}(W) \cong \mathbf{D}(\mathrm{gr}\text{-}A), \quad (57)$$

where

$$A = \frac{k[x_0, x_1, \dots, x_5]}{(f_0, f_1)}. \quad (58)$$

This equivalence leads to the identification of $\mathrm{DGrS}(W)/T_\Sigma^\Delta$ with the derived category of coherent sheaves on the complete intersection X in the Calabi–Yau phase.

Let \mathcal{O}_X be the structure sheaf of our Calabi–Yau threefold. This corresponds to the A -module A itself in $\mathbf{D}(\text{gr-}A)$. Following the algorithm of [60], \mathcal{O}_X is identified as the cokernel of the map $S(-3)^{\oplus 2} \rightarrow S$ given by (f_0, f_1) . Thus the sheaf \mathcal{O}_X is associated with the S -module \mathbf{O}_X defined as the cokernel of the map.

$$S(-3)^{\oplus 6} \xrightarrow{f_0, f_1} S \quad (59)$$

\mathbf{O}_X is an S' -module since it is annihilated by W . If we compute a free resolution of \mathbf{O}_X as an S' -module we obtain a chain complex that is infinite in length but that can be repackaged as the matrix factorization:

$$\begin{array}{ccc} S(-3) & \begin{pmatrix} f_0 & f_1 \\ -p_1 & p_0 \end{pmatrix} & S(0) \\ \oplus & \xleftrightarrow{\hspace{1cm}} & \oplus \\ S(-3) & \begin{pmatrix} p_0 & -f_1 \\ p_1 & f_0 \end{pmatrix} & S(-6)[2] \end{array} \quad (60)$$

The other key object we define is \mathbf{w} which is given by the cokernel of the map

$$S(-1)^{\oplus 6} \xrightarrow{x_0, x_1, \dots, x_5} S. \quad (61)$$

In the hybrid phase \mathbf{w} represents the structure sheaf of the zero section of the bundle of \mathbb{P}^1 . That is, \mathbf{w} represents the 2-brane wrapping \mathbb{P}^1 .

A free resolution of the S' -module \mathbf{w} is infinite in length but can be repackaged as a matrix factorization with matrices of dimension 32:

$$\begin{array}{ccc} & & S \\ & & \oplus \\ S(-1)^{\oplus 6} & & S(-2)[2]^{\oplus 15} \\ \oplus & & \oplus \\ S(-3)[2]^{\oplus 20} & \xleftrightarrow{\hspace{1cm}} & \oplus \\ \oplus & & S(-4)[4]^{\oplus 15} \\ S(-5)[4]^{\oplus 6} & & \oplus \\ & & S(-6)[6] \end{array} \quad (62)$$

Now, suppose we are in the large radius Calabi–Yau phase. We can represent the 6-brane that wraps X by \mathcal{O}_X and thus the matrix factorization (60). The object \mathbf{w} is annihilated by B_Σ and thus represents a trivial D-brane. In terms of representing the 6-brane by a matrix factorization we are free to add on (with mapping cones) arbitrary collections of \mathbf{w} 's (and its shifts in gradings) to (60). The idea of [57] is that there should be one preferred presentation of \mathcal{O}_X as an S -module that can be naturally transported into the other phase so we can identify it with matrix factorizations there. This is equivalent [16, 61] to stating that it is resolved only in terms of summands of our tilting object. That is, we only want free S -modules of the form $S(n)$, where $-5 \leq n \leq 0$. In particular, the S -module \mathbf{O}_X is *not* the preferred presentation of \mathcal{O}_X as it contains an $S(-6)$.

The trick is to find a map between \mathcal{O}_X and some grade-shifted w so that the $S(-6)$ terms cancel when we construct the mapping cone. We may introduce polynomials h_i and g_{ij} such that

$$W = \sum_{i=0}^5 h_i x_i, \quad f_j = \sum_{i=0}^5 g_{ij} x_i. \quad (63)$$

Then consider extending the following map between resolutions:

$$\begin{array}{ccccccc} \cdots & \longrightarrow & S(-5)^{\oplus 6} & \xrightarrow{h_0, \dots, h_5} & S(-6)[2] & \longrightarrow & \text{coker}(h_0, \dots, h_1) \\ & & \downarrow (g_{ji}) & & \downarrow 1 & & \\ \cdots & \longrightarrow & S(-3)^{\oplus 2} & \xrightarrow{p_0, p_1} & S(-6)[2] & \longrightarrow & \text{coker}(p_0, p_1) \end{array} \quad (64)$$

This leads to a map between the matrix factorizations above equivalent to a map $w[-4] \rightarrow \mathcal{O}_X$ which gives the necessary cancellation between the degree -6 pieces. That is, we have a triangle

$$\begin{array}{ccc} w[-4] & \longrightarrow & \mathcal{O}_X \\ & \swarrow [1] & \searrow \\ & \mathcal{Q}_X & \end{array} \quad (65)$$

or, equivalently,

$$\begin{array}{ccc} w[-3] & \xrightarrow{[1]} & \mathcal{O}_X \\ & \swarrow & \searrow \\ & \mathcal{Q}_X & \end{array} \quad (66)$$

where \mathcal{Q}_X represents the 6-brane \mathcal{O}_X in a form that can be carried into the hybrid phase.

Let us pass to the hybrid phase. Now it is \mathcal{O}_X which is annihilated by B_Σ and so \mathcal{O}_X is now trivial. In the category of D-branes in the hybrid phase the triangle (66) represents an isomorphism $\mathcal{Q}_X \cong w[-3]$. We have therefore proven

Proposition 3 *Under the equivalence between D-branes in Calabi–Yau and hybrid phases, the 6-brane corresponding to the structure sheaf \mathcal{O}_X is mapped⁴ to the matrix factorization $w[-3]$, where w is the 32×32 matrix factorization given by (62) and represents the 2-brane wrapping the \mathbb{P}^1 zero-section of the Landau–Ginzburg fibration over \mathbb{P}^1 .*

Let us denote this correspondence $\mathcal{O}_X \longleftrightarrow w[-3]$.

We could also consider a morphism

$$\begin{array}{ccccccc} \cdots & \longrightarrow & S(-1)^{\oplus 6} & \xrightarrow{x_0, \dots, x_5} & S(0) & \longrightarrow & w \\ & & \uparrow (g_{ij}) & & \uparrow 1 & & \\ \cdots & \longrightarrow & S(-3)^{\oplus 2} & \xrightarrow{f_0, f_1} & S(0) & \longrightarrow & \mathcal{O}_X \end{array} \quad (67)$$

⁴This mapping is not unique. The mapping we give here is the one dictated by the particular tilting object we use.

which would cancel out the $S(0)$'s in the mapping cone. Twisting everything by $S(1)$ this gives a triangle

$$\begin{array}{ccc} \mathbf{O}_X(1) & \longrightarrow & \mathbf{w}(1) \\ & \searrow & \swarrow [1] \\ & \mathbf{R}_X & \end{array} \quad (68)$$

where \mathbf{R}_X is an S -module that represents the sheaf $\mathcal{O}_X(1)$ in the Calabi–Yau phase in a form suitable for transport into the hybrid phase. In the hybrid phase, $\mathbf{O}_X(1)$ becomes trivial and therefore we have a correspondence

$$\mathcal{O}_X(1) \longleftrightarrow \mathbf{w}(1)[-1]. \quad (69)$$

Now consider what, in the Calabi–Yau phase would correspond to $\mathbf{w}(2)$ in the hybrid phase. Looking at (67) twisted by $S(2)$ we see that we need to get rid of $S(1)^{\oplus 6}$ and $S(2)$ to yield a resolution purely in terms of the tilting summands. We may remove the $S(2)$'s by coning with $\mathbf{O}_X(2)$ and then the six $S(1)$'s by coning with $\mathbf{O}_X(1)$'s. When we pass to the Calabi–Yau phase the $\mathbf{w}(2)$ becomes trivial and we are left with a correspondence

$$\mathbf{w}(2) \longleftrightarrow \left(\mathcal{O}_X(1)^{\oplus 6} \longrightarrow \mathcal{O}_X(2) \right) [1], \quad (70)$$

where the dotted line denotes position 0 in the complex. Let Ω^n denote the n^{th} exterior power of the cotangent sheaf of \mathbb{P}^5 and let Ω_X^n denote $\Omega^n \otimes \mathcal{O}_X$. Then the above becomes $\mathbf{w}(2) \longleftrightarrow \Omega_X^1(2)[2]$. Continuing in this fashion we get a correspondence

$$\mathbf{w}(n) \longleftrightarrow \Omega_X^{n-1}(n)[n], \quad \text{for } n = 1, 2, 3. \quad (71)$$

Note that (71) fails for $n = 4$ because maps containing p_i in (62) start to make the resolution of \mathbf{w} in (67) differ from the Koszul resolution.⁵

4.3 D-branes with moduli space \mathbb{P}^1

Consider a \mathbb{P}^1 with homogeneous coordinate ring $S = k[x_0, x_1]$ and let p be a point in this curve with homogeneous coordinates $[u_0, u_1]$. If \mathcal{O} is the structure sheaf of the curve and \mathcal{O}_p is the skyscraper sheaf of p we have a short exact sequence

$$0 \longrightarrow \mathcal{O}(-1) \xrightarrow{u_0 x_0 + u_1 x_1} \mathcal{O} \longrightarrow \mathcal{O}_p \longrightarrow 0. \quad (72)$$

The variables p_0 and p_1 in the homogeneous coordinate ring serve as the homogeneous coordinates of \mathbb{P}^1 in the hybrid phase. We already know that \mathbf{w} represents the structure sheaf of this \mathbb{P}^1 . Let p be a point on this \mathbb{P}^1 with homogeneous coordinates $[u_0, u_1]$ and let

⁵This fact ruins any hope of finite monodromy around this limit that would have been seen in, for example, the Landau-Ginzburg phase of the quintic.

\mathcal{P}_p be the cokernel of a linear combination of these coordinates corresponding to the point p . Given that p has charge $(2, -3)$, we have a triangle

$$\begin{array}{ccc} & \mathcal{P}_p & \\ \swarrow [1] & & \nwarrow \\ \mathbf{w}(3)[-2] & \xrightarrow{u_0 p_0 + u_1 p_1} & \mathbf{w} \end{array} \quad (73)$$

as the analogue of (72). Thus \mathcal{P}_p is the natural candidate for a brane to probe the geometry of the \mathbb{P}^1 .

From the previous section we know we may rephrase (73) in terms of $\mathbf{D}(X)$ as

$$\begin{array}{ccc} & \mathcal{P}_p & \\ \swarrow [1] & & \nwarrow \\ \Omega_X^2(3)[1] & \xrightarrow{u_0 p_0 + u_1 p_1} & \mathcal{O}_X[3] \end{array} \quad (74)$$

It is important to note that it would be misleading to call \mathcal{P}_p a 0-brane. Looking at (74) it is not hard to see that the K-theory class of \mathcal{P}_p is not equal to that of a point. We need a different D-brane to “see” the \mathbb{P}^1 . In all probability, the true 0-brane probes remain stable everywhere in the moduli space (so long as we don’t cross branch cuts) and so the geometry by this criterion is always X .

In order for \mathcal{P}_p to see the geometry of the \mathbb{P}^1 , it must be stable. At large radius limit, the phase of a coherent sheaf is given by

$$\xi(\mathcal{E}) = -\frac{1}{2} \dim \text{supp}(\mathcal{E}). \quad (75)$$

It follows that

$$\xi(\mathcal{O}_X[3]) - \xi(\Omega_X^2(3)[1]) = 2, \quad (76)$$

and so (assuming these sheaves are stable) \mathcal{P}_p is *unstable* from (74).

So, at the large radius limit, evidence of the \mathbb{P}^1 of the hybrid phase does not exist. Naturally we would like to know if it appears as we move towards the hybrid phase. Lacking a practical rigorous stability criterion we will just consider the triangle (74) to determine when \mathcal{P}_p is stable.

We need to determine the exact values of the phases ξ as we move in the moduli space of $B + iJ$. This is very similar to the analysis of the quintic done in [44]. Since $h^{1,1}(X) = 1$, let $B + iJ = tx$, where x is dual to the divisor class $x_0 = 0$ in X .

Introduce the algebraic coordinate

$$z = \frac{\tilde{a}_1 \tilde{a}_2 \tilde{a}_3 \tilde{a}_4 \tilde{a}_5 \tilde{a}_6}{\tilde{p}_0^3 \tilde{p}_1^3}. \quad (77)$$

The periods then solve the Picard–Fuchs equation $\square\Phi = 0$, where

$$\square = \left(z \frac{\partial}{\partial z}\right)^4 - 27^2 z \left(z \frac{\partial}{\partial z} + \frac{1}{3}\right)^2 \left(z \frac{\partial}{\partial z} + \frac{2}{3}\right)^2. \quad (78)$$

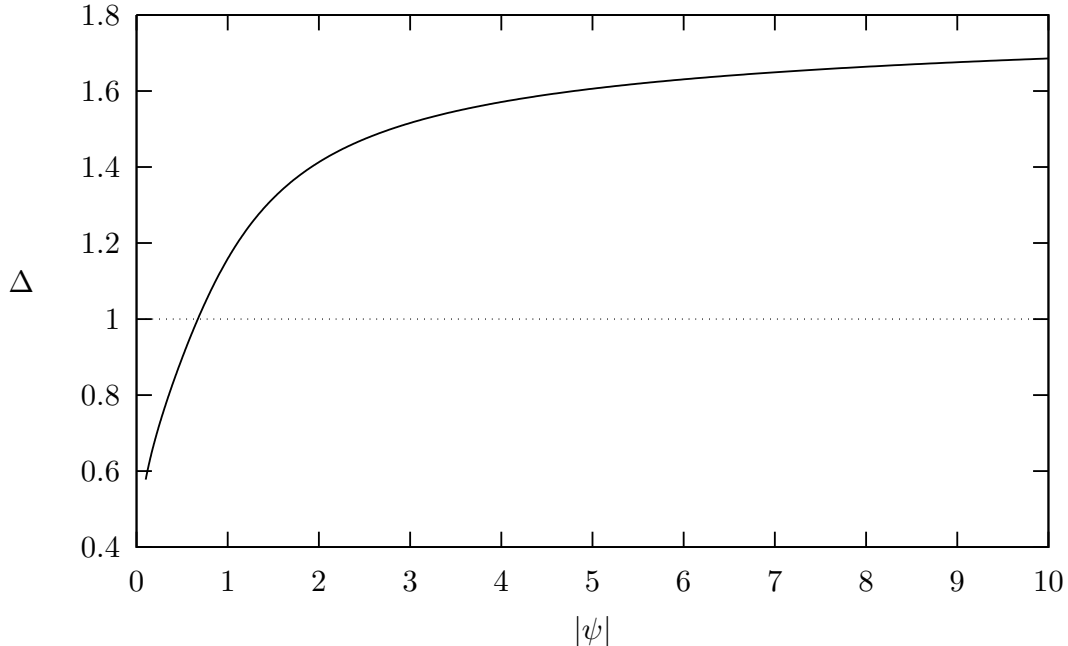


Figure 6: Difference in phases for decay of \mathcal{P}_p on \mathbb{P}^1 .

It is useful to put $z = (9\psi)^{-3}$, where $\psi = 0$ in the limit of the hybrid phase.

The central charges of the line bundles $\mathcal{O}(n)$ are then given by

$$\begin{aligned} Z(\mathcal{O}(n)) &= \int_X e^{-tx} e^{nx} (1 + \frac{1}{4}x^2) + \dots \\ &= -\frac{3}{4}(t-n)(2t^2 - 4tn + 3 + 2n^2) + \dots, \end{aligned} \tag{79}$$

which allows them to be identified in periods as was done in [30, 44].

A lengthy numerical computation then yields the difference in the phases $\Delta = \xi(\mathcal{O}_X[3]) - \xi(\Omega_X^2(3)[1])$ as a function of ψ . In figure 6 we plot how Δ varies with $|\psi|$ where we set $\arg(\psi) = -i\pi/3$ to keep away from branch cuts. One sees that for sufficiently small $|\psi|$, $\Delta < 1$ and so \mathcal{P}_p is stable relative to the triangle (74).

Of course to be rigorous we need to consider *all* possible triangles. We also need to be sure that both \mathcal{O}_X and $\Omega_X^2(3)$ are stable when we apply our criterion for stability. We cannot address either of these issues rigorously but one should note that both \mathcal{O}_X and $\Omega_X^2(3)$ are “fractional branes” that become massless and induce singularities in the conformal field theory and some points in the moduli space. We therefore know that they are stable “nearby” in some sense. Anyway, we will assume that the only triangle needed for checking stability is (74).

Assume first $\Delta < 1$ in figure 6. Then $u_0 = u_1 = 0$, corresponding to $\mathcal{P}_p = \Omega_X^2(3)[2] \oplus \mathcal{O}_X[3]$, is unstable, and we have an obvious \mathbb{C}^* -action, $(u_0, u_1) \rightarrow (\lambda u_0, \lambda u_1)$, yielding isomorphism classes of \mathcal{P}_p . The moduli space of \mathcal{P}_p is thus \mathbb{P}^1 . If $\Delta = 1$ then $\mathcal{P}_p =$

$\Omega_X^2(3)[2] \oplus \mathcal{O}_X[3]$ is polystable and no nonzero values of u_0 or u_1 yield polystable objects so the moduli space of \mathcal{P}_p is a point. Thus at $\Delta = 1$ the \mathbb{P}^1 shrinks to a point and for $\Delta > 1$ we have no \mathbb{P}^1 at all.

So we do seem to have a D-brane probe whose moduli space is the \mathbb{P}^1 base of the hybrid. It would appear then, that in the hybrid phase both the original 0-brane \mathcal{O}_p and this new D-brane probe \mathcal{P}_p are stable. One of them, \mathcal{O}_p , has a moduli space given by the Calabi–Yau threefold while the other, \mathcal{P}_p has a moduli space of \mathbb{P}^1 .

5 Discussion

In sections 2, 3 and 4 we considered shrinking, respectively, a curve, a divisor and the whole threefold. As one might expect from the naïve angle argument from the beginning of section 3, we see roughly that 0-brane decay happens as we pass between phases, as we hit the limit of a phase or never, respectively.

In addition, in the hybrid case we could find a D-brane whose moduli space was \mathbb{P}^1 so long as we remained in the hybrid phase. This is consistent with the point of view that a shrinking \mathbb{P}^1 supports no stable “0-branes” as we pass beyond the phase boundary. This suggests a nice resolution of the fact that this model is both 3-dimensional and 1-dimensional.

In the exoflop case we saw that the 0-brane probe never sees the external \mathbb{P}^1 . Presumably, from the results of section 4, there is another D-brane which does probe this \mathbb{P}^1 correctly so long as we are in the exoflop phase. That is, just like the hybrid case, we need two different D-brane charges to fully probe the geometry. It would be interesting to find this expected extra D-brane.

Aside from this expected result there are some surprising results coming from finite volume effects. We recover, from a brane probe point of view, the minimum distance idea of [6] that exceptional divisors can only be shrunk down to zero size if the volume of the Calabi–Yau threefold is infinitely large. This turns out to be quite a surprise in the extremal transition case since this results in an even more discontinuous change in geometry than expected for a topology transition. It would be very interesting to see exactly what happens to this discontinuity when the string coupling is turned on.

Acknowledgments

I wish to thank S. Guerra, I. Melnikov, R. Plesser and A. Roy for useful discussions. The author is supported by an NSF grant DMS–0606578.

References

- [1] E. Witten, *D-branes and K-Theory*, J. High Energy Phys. **12** (1998) 019, hep-th/9810188.

- [2] T. Bridgeland, *Flops and Derived Categories*, math.AG/0009053.
- [3] M. R. Douglas, B. Fiol, and C. Römelsberger, *Stability and BPS Branes*, hep-th/0002037.
- [4] E. Witten, *Phases of $N = 2$ Theories in Two Dimensions*, Nucl. Phys. **B403** (1993) 159–222, hep-th/9301042.
- [5] P. S. Aspinwall, B. R. Greene, and D. R. Morrison, *Measuring Small Distances in $N = 2$ Sigma Models*, Nucl. Phys. **B420** (1994) 184–242, hep-th/9311042.
- [6] P. S. Aspinwall, *Minimum Distances in Non-Trivial String Target Spaces*, Nucl. Phys. **B431** (1994) 78–96, hep-th/9404060.
- [7] E. Witten, *Phase Transitions in M-Theory and F-Theory*, Nucl. Phys. **B471** (1996) 195–216, hep-th/9603150.
- [8] A. C. Avram, P. Candelas, D. Jančić, and M. Mandelberg, *On the Connectedness of Moduli Spaces of Calabi–Yau Manifolds*, Nucl. Phys. **B465** (1996) 458–472, hep-th/9511230.
- [9] B. R. Greene, D. R. Morrison, and A. Strominger, *Black Hole Condensation and the Unification of String Vacua*, Nucl. Phys. **B451** (1995) 109–120, hep-th/9504145.
- [10] A. Caldararu et al., *Non-Birational Twisted Derived Equivalences in Abelian GLSMs*, arXiv:0709.3855.
- [11] M. R. Douglas, *D-Branes, Categories and $N=1$ Supersymmetry*, J. Math. Phys. **42** (2001) 2818–2843, hep-th/0011017.
- [12] P. S. Aspinwall, *A Point’s Point of View of Stringy Geometry*, JHEP **01** (2003) 002, hep-th/0203111.
- [13] D. A. Cox, *The Homogeneous Coordinate Ring of a Toric Variety*, J. Algebraic Geom. **4** (1995) 17–50, alg-geom/9210008.
- [14] A. A. Beilinson, *Coherent Sheaves on \mathbb{P}^n and Problems in Linear Algebra*, Func. Anal. Appl. **12** (1978) 214–216.
- [15] I. R. Klebanov and E. Witten, *Superconformal Field Theory on Threebranes at a Calabi–Yau Singularity*, Nucl. Phys. **B536** (1998) 199–218, hep-th/9807080.
- [16] P. S. Aspinwall, *D-Branes on Toric Calabi–Yau Varieties*, arXiv:0806.2612.
- [17] T. Bridgeland, *Stability Conditions on a Non-Compact Calabi–Yau Threefold*, Commun. Math. Phys. **266** (2006) 715–733, arXiv:math/0509048.
- [18] A. Bergman, *A Note on Support in Triangulated Categories*, arXiv:0804.3986.

- [19] P. S. Aspinwall and I. V. Melnikov, *D-branes on Vanishing del Pezzo Surfaces*, JHEP **12** (2004) 042, hep-th/0405134.
- [20] A. V. Sardo Infirri, *Resolutions of Orbifold Singularities and the Transportation Problem on the McKay Quiver*, alg-geom/9610005.
- [21] M. R. Douglas, B. R. Greene, and D. R. Morrison, *Orbifold Resolution by D-Branes*, Nucl. Phys. **B506** (1997) 84–106, hep-th/9704151.
- [22] S. Franco and D. Vegh, *Moduli spaces of gauge theories from dimer models: Proof of the correspondence*, JHEP **11** (2006) 054, hep-th/0601063.
- [23] A. Ishii and K. Ueda, *On Moduli Spaces of Quiver Representations Associated with Dimer Models*, arXiv:0710.1898.
- [24] A. Bergman and N. J. Proudfoot, *Moduli Spaces for Bondal Quivers*, Pacific J. Math. **237** (2008) 201–221, arXiv:math/0512166.
- [25] A. D. King, *Moduli of Representations of Finite Dimensional Algebras*, Quart. J. Math. Oxford (2) **45** (1994) 515–530.
- [26] M. R. Douglas, B. Fiol, and C. Romelsberger, *The Spectrum of BPS Branes on a Noncompact Calabi-Yau*, hep-th/0003263.
- [27] M. Lieblich, *Moduli of Complexes on a Proper Morphism*, J. Alg. Geom. **15** (2006) 175–206, arXiv:math/0502198.
- [28] A. Bayer, *Polynomial Bridgeland Stability Conditions and the Large Volume Limit*, arXiv:0712.1083.
- [29] D. R. Morrison and M. R. Plesser, *Non-Spherical Horizons. I*, Adv. Theor. Math. Phys. **3** (1999) 1–81, hep-th/9810201.
- [30] P. S. Aspinwall, *D-Branes on Calabi-Yau Manifolds*, in J. M. Maldacena, editor, “Progress in String Theory. TASI 2003 Lecture Notes”, pages 1–152, World Scientific, 2005, hep-th/0403166.
- [31] T. Bridgeland, *Stability Conditions on Triangulated Categories*, math.AG/0212237.
- [32] A. Bergman, *Stability Conditions and Branes at Singularities*, JHEP **10** (2008) 073, hep-th/0702092.
- [33] S. Donaldson, *Anti-Self-Dual Yang-Mills Connections on Complex Algebraic Surfaces and Stable Vector Bundles*, Proc. London Math Soc. **50** (1985) 1–26.
- [34] K. Uhlenbeck and S.-T. Yau, *On the Existence of Hermitian Yang-Mills Connections in Stable Vector Bundles*, Commun. Pure App. Math. **39** (1986) S257–S293.

- [35] R. P. Horja, *Derived Category Automorphisms from Mirror Symmetry*, math.AG/0103231.
- [36] P. S. Aspinwall, R. L. Karp, and R. P. Horja, *Massless D-branes on Calabi-Yau threefolds and monodromy*, Commun. Math. Phys. **259** (2005) 45–69, hep-th/0209161.
- [37] P. Candelas et al., *Mirror Symmetry for Two Parameter Models — I*, Nucl. Phys. **B416** (1994) 481–562, hep-th/9308083.
- [38] P. Candelas, A. Font, S. Katz, and D. R. Morrison, *Mirror Symmetry for Two Parameter Models — II*, Nucl. Phys. **B429** (1994) 626–674, hep-th/9403187.
- [39] P. S. Aspinwall, B. R. Greene, and D. R. Morrison, *Multiple Mirror Manifolds and Topology Change in String Theory*, Phys. Lett. **303B** (1993) 249–259.
- [40] V. V. Batyrev, *Dual Polyhedra and Mirror Symmetry for Calabi–Yau Hypersurfaces in Toric Varieties*, J. Alg. Geom. **3** (1994) 493–535.
- [41] P. S. Aspinwall, B. R. Greene, and D. R. Morrison, *The Monomial-Divisor Mirror Map*, Internat. Math. Res. Notices **1993** 319–338, alg-geom/9309007.
- [42] D. R. Morrison and M. R. Plesser, *Summing the Instantons: Quantum Cohomology and Mirror Symmetry in Toric Varieties*, Nucl. Phys. **B440** (1995) 279–354, hep-th/9412236.
- [43] P. S. Aspinwall, *D-branes, Pi-stability and Theta-stability*, in “Snowbird Lectures on String Geometry”, AMS, 2006, hep-th/0407123.
- [44] P. S. Aspinwall and M. R. Douglas, *D-Brane Stability and Monodromy*, JHEP **05** (2002) 031, hep-th/0110071.
- [45] M. Kreuzer and H. Skarke, *PALP: A Package for Analyzing Lattice Polytopes with Applications to Toric Geometry*, Comput. Phys. Commun. **157** (2004) 87–106, arXiv:math/0204356.
- [46] F. Cachazo, B. Fiol, K. A. Intriligator, S. Katz, and C. Vafa, *A Geometric Unification of Dualities*, Nucl. Phys. **B628** (2002) 3–78, hep-th/0110028.
- [47] C. P. Herzog, *Exceptional Collections and del Pezzo Gauge Theories*, hep-th/0310262.
- [48] D. Berenstein and M. R. Douglas, *Seiberg Duality for Quiver Gauge Theories*, hep-th/0207027.
- [49] D. L. Jafferis and G. W. Moore, *Wall Crossing in Local Calabi–Yau Manifolds*, arXiv:0810.4909.
- [50] L. Borisov, *Towards the Mirror Symmetry for Calabi–Yau Complete Intersections in Gorenstein Toric Fano Varieties*, alg-geom/9310001.

- [51] P. S. Aspinwall and B. R. Greene, *On the Geometric Interpretation of $N = 2$ Superconformal Theories*, Nucl. Phys. **B437** (1995) 205–230, hep-th/9409110.
- [52] J. Walcher, *Stability of Landau–Ginzburg Branes*, J. Math. Phys. **46** (2005) 082305, hep-th/0412274.
- [53] I. Brunner and M. R. Gaberdiel, *Matrix Factorisations and Permutation Branes*, JHEP **07** (2005) 012, hep-th/0503207.
- [54] A. Kapustin and Y. Li, *D-branes in Landau-Ginzburg Models and Algebraic Geometry*, JHEP **12** (2003) 005, hep-th/0210296.
- [55] D. Orlov, *Derived Categories of Coherent Sheaves and Triangulated Categories of Singularities*, math.AG/0503632.
- [56] P. S. Aspinwall, *Topological D-Branes and Commutative Algebra*, hep-th/0703279, submitted to Communications in Number Theory and Physics.
- [57] M. Herbst, K. Hori, and D. Page, *Phases Of $N = 2$ Theories In $1 + 1$ Dimensions With Boundary*, arXiv:0803.2045.
- [58] D. Eisenbud, *Homological Algebra on a Complete Intersection, with an Application to Group Representations*, Trans. Amer. Math. Soc. **260** (1980) 35–64.
- [59] T. H. Gulliksen, *A Change of Ring Theorem with Applications to Poincare Series and Intersection Multiplicity*, Math. Scand. **34** (1974) 167–183.
- [60] L. L. Avramov and D. R. Grayson, *Resolutions and Cohomology over Complete Intersections*, in D. Eisenbud et al., editors, “Computations in Algebraic Geometry with Macaulay 2”, Algorithms and Computations in Mathematics **8**, pages 131–178, Springer-Verlag, 2001.
- [61] M. Van den Bergh, *Non-Commutative Crepant Resolutions*, in “The Legacy of Niels Henrik Abel: The Abel Bicentennial, Oslo 2002”, pages 749–770, Springer, 2004, arXiv:math/0211064.